Accepted Manuscript

Design, synthesis and preliminary bioactivity evaluations of 8-hydroxyquinoline derivatives as matrix metalloproteinase (MMP) inhibitors

Chen Chen, Xinying Yan, Hao Fang, Xuben Hou

PII: S0223-5234(19)30687-7

DOI: https://doi.org/10.1016/j.ejmech.2019.111563

Article Number: 111563

Reference: EJMECH 111563

To appear in: *European Journal of Medicinal Chemistry*

Received Date: 19 April 2019

Revised Date: 23 July 2019

Accepted Date: 23 July 2019

Please cite this article as: C. Chen, X. Yan, H. Fang, X. Hou, Design, synthesis and preliminary bioactivity evaluations of 8-hydroxyquinoline derivatives as matrix metalloproteinase (MMP) inhibitors, *European Journal of Medicinal Chemistry* (2019), doi: https://doi.org/10.1016/j.ejmech.2019.111563.

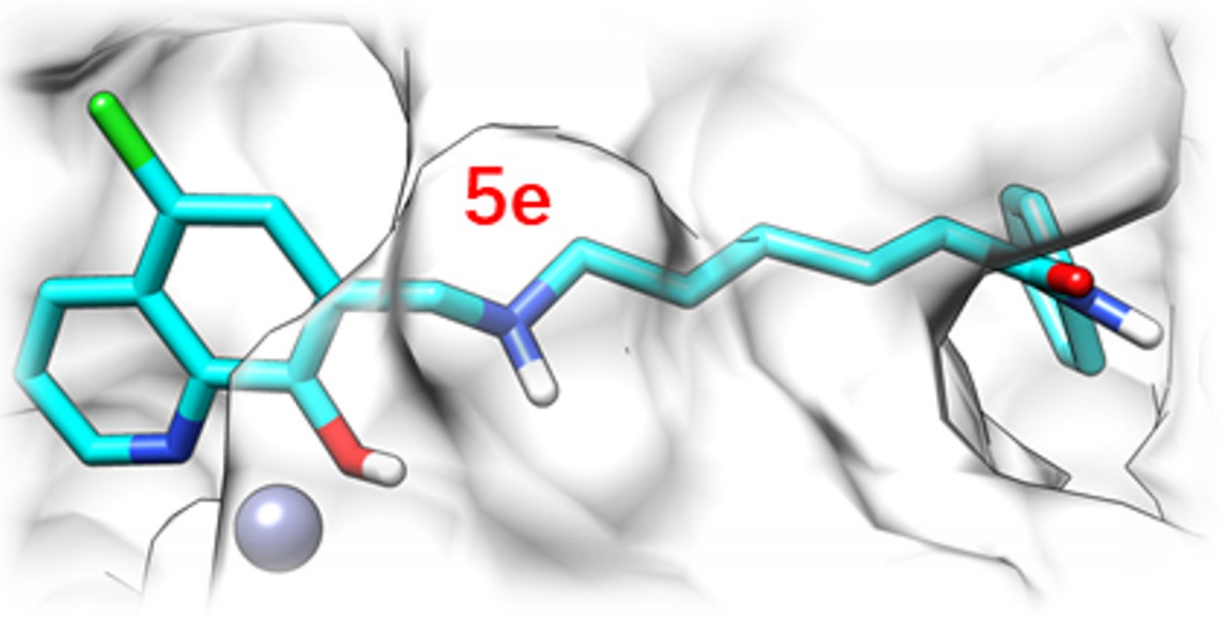

Cpd.	MMP-2 IC_{50}(μM)	MMP-9 IC_{50}(μM)
5e	0.70±0.02	0.66±0.01

Design, synthesis and preliminary bioactivity evaluations of 8-hydroxyquinoline derivatives as matrix metalloproteinase (MMP) inhibitors

Chen Chen [a], Xinying Yang [a], Hao Fang [a], Xuben Hou [a, *]

[a] *Department of Medicinal Chemistry, Key Laboratory of Chemical Biology (Ministry of Education), School of Pharmaceutical Sciences, Shandong University, 44 West Culture Road, 250012, Jinan, Shandong, PR China*

***Address correspondence to this author:**
Prof. Xuben Hou, Department of Medicinal Chemistry, School of Pharmaceutical Sciences, Shandong University, 44 West Wenhua Road, Jinan, PR China.
E-mail: hxb@sdu.edu.cn
Tel. 86-531-88382009
Fax. 86-531-88382548

Abstract: Matrix metalloproteinases (MMPs) play important roles in many diseases including cancer. With moderate metal-binding affinity, 8-hydroxyquinoline has gained much interest in current drug design and development. Specially, it has been reported that 8-hydroxyquinoline derivatives serve as MMP-2 inhibitors with micromolar IC_{50} values. In the current study, a series of 8-hydroxyquinoline derivatives were designed and synthesized as new MMP-2 and MMP-9 inhibitors. The most active compounds **5e** and **5h** not only displayed good inhibitory activities against MMP-2/9 with IC_{50} at submicromolar level, but also possessed potent anti-proliferative, anti-invasive and anti-angiogenesis activity in A549 cell line. Western blot also revealed that **5e** and **5h** down-regulate the expression of MMP-2 and MMP-9 in A549 cell line. Moreover, flow cytometry analysis indicated that compound **5e** could promote apoptosis of A549 cells *in vitro*. Molecular docking analysis also revealed favorable binding modes of **5e** in the active sites of MMP-2 and MMP-9.

Keywords:
8-hydroxyquinoline
MMP-2/9 inhibitors
Anti-migration/invasion
Anti-angiogenesis

1. Introduction

Matrix metalloproteases (MMPs) are zinc-dependent endopeptidases that proteolytically degrade various components of the extracellular matrix (ECM). To date, at least 24 MMPs have been identified in human, which could be classified into five subfamilies based on their specificities [1]. Among various MMPs, MMP-2 and MMP-9 (also known as gelatinase A and B) serve as important gelatinases. The structures of both MMP-2 and MMP-9 consist of an N-terminal predomain, a prodomain and a catalytic domain with a zinc-binding site (**Fig. 1**). The predomain could guide gelatinases to the endoplasmic reticulum and the prodomain could maintain the latency of the gelatinases. The catalytic domain of MMP-2 and MMP-9 also comprises three repeatedly collagen-binding type II of fibronectin (Fi) inserts.

Fig. 1. Structures of MMP-2 and MMP-9.

MMP-2 and MMP-9 play critical roles in tumor proliferation, migration, invasion and angiogenesis. For example, MMP-2 and MMP-9 could induce the release of cell-membrane-precursors of growth factors, such as insulin-like growth factors (IGFs) and epidermal growth factor receptor (EGFR) ligands, which promote tumor proliferation [2]. Moreover, MMP-2 and MMP-9 could regulate proliferation signals by shedding and activating the transforming growth factor TGF-β [3]. The ECM is a natural barrier that prevents tumor cell invasion and metastasis [4]. Since MMP-2 and MMP-9 exert proteolytic activities and degrade physical barriers, developing MMP-2/9 inhibitors should prevent tumor cell invasion and metastasis. During tumor angiogenesis progression, MMP-2 and MMP-9 play critical roles through participating in the degradation of the vascular basement membrane and remodeling of the ECM [5]. MMP-2 and MMP-9 are also known as "angiogenic switches" which promote tumor vascularization [6]. Expression of both MMP-2 and MMP-9 are upregulated in angiogenic lesions. MMP-9 can release VEGF to render normal islets angiogenic [7]. When the MMP-2 expression is down-regulated by antisense oligonucleotides, tumor cells lose their angiogenic ability and tumor growth is inhibited [8]. It had been reported that MMP inhibitors could induce cell apoptosis [9, 10] and down-regulate MMP-2 or MMP-9 expression [9]. For example, previously reported MMP-2/9 inhibitor could interact synergistically with ligands of the TNF receptor superfamily to induce apoptosis in a cell-type-specific manner [11]. Therefore, inhibition of MMP-2/9 serves as a potentially valuable strategy for anti-cancer drug design and development.

Hydroxamic acids derivatives are the most common MMPs inhibitors, however, several hydroxamate-based MMP inhibitors failed in clinical trial due to low isoform selectivity and various toxicities, such as joint stiffness, swelling and arthralgia[12]. Currently, development of non-hydroxamate inhibitors against specific MMPs is of foremost interest. 8-Hydroxyquinoline is an important scaffold in drug development [13] and its derivatives (e.g. Clioquinol) have already been used in clinical therapy [14]. Previously, Jacobsen and coworkers screened hundreds of fragments and found that 8-hydroxyquinoline possessed inhibitory activity against MMPs [15].

Further structural modification suggested that aromatic substitutions at either the 5- or 7-positions of 8-hydroxyquinoline could yield MMP-2 inhibitors (Compound **A** and **B** in **Fig. 2**).

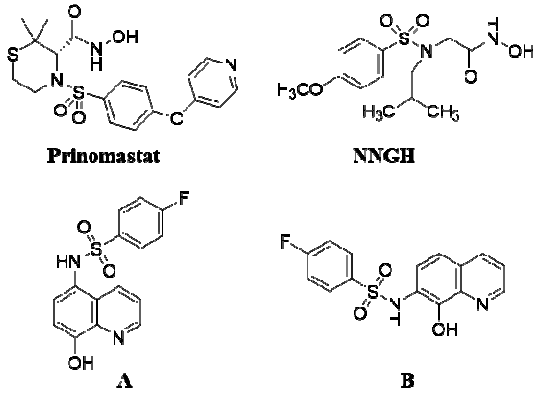

Fig. 2. Reported MMP inhibitors.

As far as the structure of MMPIs is concerned, it should contain a zinc binding group and a chemical moiety protruding into the deep and hydrophobic S1' pocket [16]. For instance, known MMP inhibitor **NNGH** (Fig.2, MMP-8, -9, -12, -13, and -20 with K_i values of 9, 2.6, 4.3, 3.1, and 17 nM, respectively) mainly interacts with the S1' pocket[17]. Docking analysis (**Fig. 3**) suggested that 8-hydroxyquinoline chelated the zinc ion and lead compound **B** is surrounded by less occupied pockets (e.g. S1' pocket and S1 pocket). Inspired by these analyses above, we designed a new series of MMP inhibitors using 8-hydroxyquinoline as the zinc binding group. Flexible linkers with different lengths were introduced between 8-hydroxyquinoline and aromatic substitutions of quinoline to improve interactions with these pockets, especially interactions with S1' pocket. This paper describes the synthesis and evaluation of these compounds, as well as their effects on cancer proliferation, migration, angiogenesis and apoptosis.

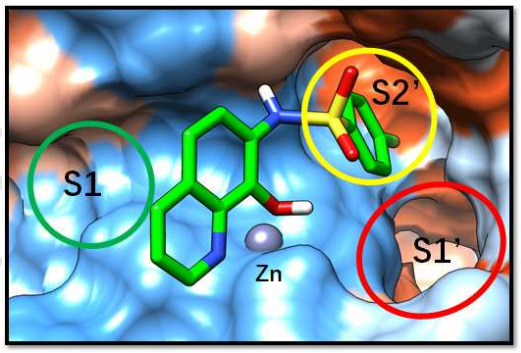

Fig. 3. Predicted binding mode of compound **B** against MMP-2.

2. Results and discussion

2.1. Chemistry

The synthetic routes of all target compounds are outlined in Schemes 1 and 2. As shown in Scheme 1, commercially available starting materials **1a**-**1e** were protected with a Boc group and then coupled with different amines. Amides **3a**-**3j** were converted to intermediates **4a**-**4j** by deprotection of the amine. Amines **4a**-**4j** were synthesized according to literatures [18, 19]. Then, compounds **4a**-**4j** were reacted with 5-chloro-8-hydroxyquinoline-7-carbaldehyde or

8-hydroxyquinoline-5-carbaldehyde *via* reductive amination to obtain target compounds **5a-5s**. As shown in Scheme 2, compound **7** was synthesized by protecting the OH group of **6**. Compounds **9a-9f** were afforded *via* **8a-f** reacting with N-methylaniline, 2-methylbenzimidazole and saccharin according to published literatures [20-22]. Intermediate **7** underwent a coupling reaction with **9a-f** to provide **10a-11i**. Deprotection of the TBS group yielded the target compounds **11a-11i**.

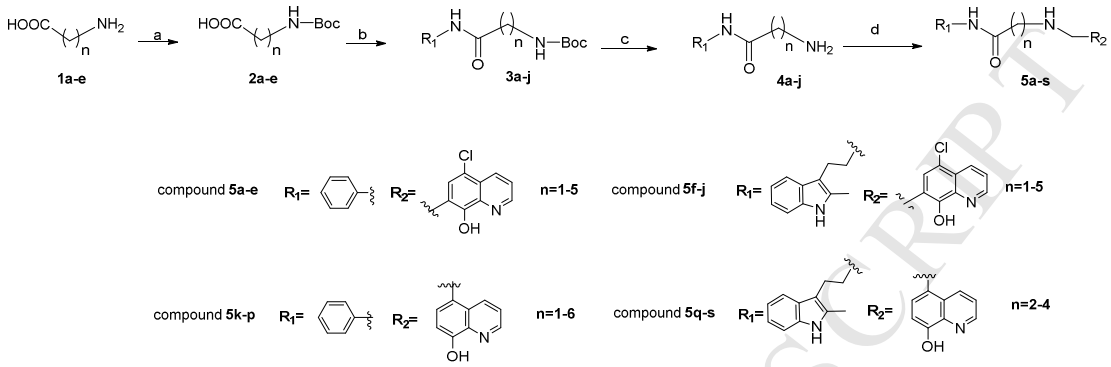

Scheme 1. Synthesis of target compounds **5a-s**. Reagents and conditions: (a) $(Boc)_2O$, 1,4-dioxane, 1M aq NaOH, rt, 8h; (b) R_1-NH_2, EDCI, HOBT, DCM, rt, 6h; (c) HCl-AcOEt (d) 5-chloro-8-hydroxyquinoline-7-carbaldehyde or 8-hydroxyquinoline-5-carbaldehyde, MeOH, rt, 4h; $NaBH_4$, rt, 1h.

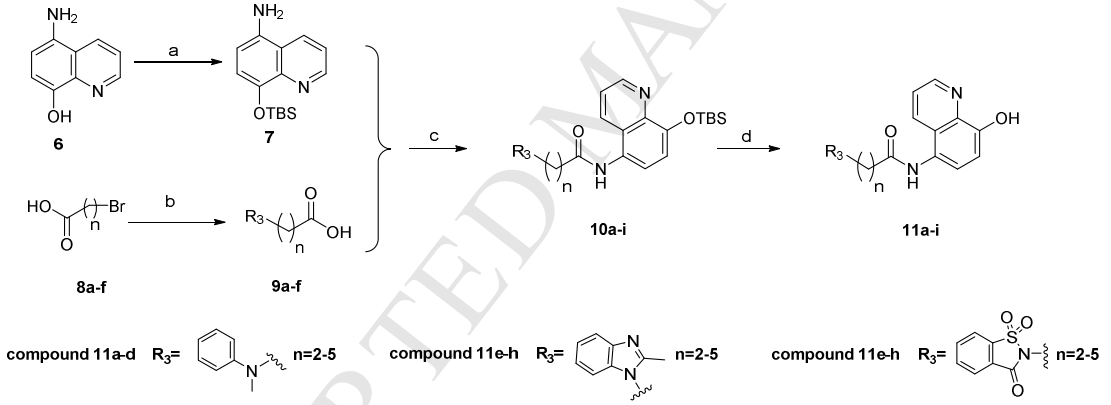

Scheme 2. Synthesis of target compounds **11a-i**. Reagents and conditions: (a) TBSCl, imidazole, DCM; (b) R_3-H, K_2CO_3, DMF, rt or 120□; (c) oxalyl chloride, DCM, rt, 1h; $NaHCO_3$, DCM, rt, 5h; (d) HCl, MeOH.

2.2. MMP-2 and MMP-9 inhibitory activity

The inhibitory activities against MMP-2 and MMP-9 of these quinoline derivatives were determined using Colorimetric Drug Discovery Kit (BML-AK408, BML-AK410, Enzo®Life Sciences). Known MMP inhibitors (Compound **A** [15], **NNGH** [23] and **Prinomastat** [12]) were used as positive control. As shown in Table 1, target compounds with aromatic substitutions at the 5-positions of quinoline are ineffective against MMP-2 and MMP-9, with only **5m**, **5o**, **5s**, **11c** and **11d** exhibiting obvious MMP inhibition (IC_{50} < 10 μM). In contrast, compounds **5a-5j**, which possess aromatic substitutions at the 7-positions, showed good inhibitory activities against MMP-2 and MMP-9. In addition, it seems that the various lengths of linkers have different influence on MMP inhibitory activity. For compounds **5a-5e**, **5e** with five-methylene linker displayed the most potent inhibitory activity against MMP-2. Among compounds **5f-5j**, compound

5h with three-methylene linker showed the best inhibitory activity with lowest IC_{50} values. These results revealed the importance of a suitable linker length in the inhibition of MMPs.

It should be noted that **5e** and **5h** are inhibitors of both MMP-2 and MMP-9 with IC_{50} values ranging from 0.66 μM to 1.23 μM. On the other hand, compound **11c** and **11d** displayed selectivity of MMP-2 over MMP-9 (more than 7-fold). The IC_{50} values of **11c** and **11d** against MMP-2 are 7.46 μM and 6.22 μM, whereas their inhibition ratios for MMP-9 are 35% and 26% at 50 μM (Supplementary material Table S2).

Table. 1. IC_{50} values of target compounds against MMP-2 and MMP-9.

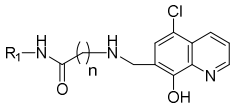

5a-5j

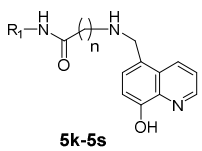

5k-5s

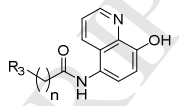

11a-11l

Cpd.	R_1	n	MMP-2 IC_{50}[a](μM)	MMP-9 IC_{50}[a](μM)
5a	Ph-	1	3.2±0.52	2.1±0.33
5b	Ph-	2	3.3±0.01	3.5±0.01
5c	Ph-	3	3.8±0.48	3.2±0.09
5d	Ph-	4	3.0±0.57	3.6±0.21
5e	Ph-	5	0.70±0.02	0.66±0.01
5f		1	8.8±0.34	>10
5g		2	>10	>10
5h		3	0.81±0.14	1.3±0.09
5i		4	7.6±0.76	3.1±0.05
5j		5	3.6±0.50	1.7±0.48
5k	Ph-	1	>10	>10
5l	Ph-	2	>10	>10
5m	Ph-	3	5.7±1.1	5.1±0.30
5n	Ph-	4	>10	>10
5o	Ph-	5	8.8±0.19	6.0±0.21
5p	Ph-	6	>10	>10
5q		2	>10	>10
5r		3	>10	>10
5s		4	8.8±0.19	5.3±0.14
A			8.8±0.21	11±0.47
NNGH			0.0091±0.0021	0.0088±0.0016
Prinomastat			0.0018±0.00034	0.0033±0.00017

Cpd.	R_3	n	MMP-2 IC_{50}[a](μM)	MMP-9 IC_{50}[a](μM)
11a		2	>10	>10
11b		3	>10	>10
11c		4	7.5±0.60	>10
11d		5	6.2±0.83	>10
11e		2	>10	>10
11f		3	>10	>10
11g		4	>10	>10
11h		5	>10	>10
11i		2	>10	>10
11j		3	>10	>10
11k		4	>10	>10
11l		5	>10	>10

[a] IC_{50} were expressed as the mean ± standard deviation of three separate determinations

2.3. Molecular docking study

Molecular docking studies were performed to investigate the binding modes of our new inhibitors in the active sites of MMP-2 and MMP-9. The most potent MMP-2/9 inhibitor compound **5e** displayed favorable interactions with both MMP-2 and MMP-9 (**Fig. 4** and **Fig. 5**).

In the case of MMP-2 (**Fig. 4**), the 8-hydroxyquinoline of **5e** chelates the zinc ion through the N atom and the OH group. Importantly, the 6-(methyleneamino)-N-phenylhexanamide of **5e** inserted into the hydrophobic S1' pocket of MMP-2 enzyme formed by Leu82, Leu83, Tyr142, Ile141, Pro140, Ala139 and Leu116. In addition, hydrogen bond interactions could be found between compound **5e** and amino acid residues at the enzyme active site (Ala139 and Arg149). Regarding the docking result of **5e** with MMP-9 (**Fig. 5**), the 8-hydroxyquinoline also chelates with zinc ion. The side chain of **5e** could enter into the hydrophobic S1' pocket surrounded by amino acid residues Leu397, Tyr420, Leu188 and Glu402. Hydrogen bonds with Glu402 of MMP-9 were observed in the predicted **5e**-MMP-9 complex. Some literatures reported that the big and hydrophobic S1' pocket was more important for MMP inhibition than the small S2' pocket [16]. Compared with the predicted binding mode of compound **B** (**Fig. 3**), the improved MMPs inhibition activity of **5e** may come from its good interactions with the S1' pockets.

Moreover, we predicted the binding modes of **5b** and **5d** in MMP-2. As shown in **Fig. 6**, compounds **5b** and **5d** only partially occupy the S1' pocket due to their shorter linkers. Moreover, the interactions between 8-hydroxyquinoline and zinc ion in **5b** and **5d** are weaker than **5e** (**Fig. 6**). These results would be helpful to understand the better MMP inhibitory activity of **5e** than **5b** and **5d**. Furthermore, we performed molecular docking of **11c** with MMP-2 and MMP-9 to investigate its isoform selectivity. According to the calculated docking scores, the predicted binding affinity of **11c** with MMP-2 (docking score=7.32) is higher than MMP-9 (docking score=4.98), possibly due to the good interactions between **11c** and S1' pocket in MMP-2 (Supplementary material, Figure S1). This result may explain the reason why **11c** was more potent for MMP-2 (IC_{50} =7.5 μM) than MMP-9 (IC_{50} >50μM).

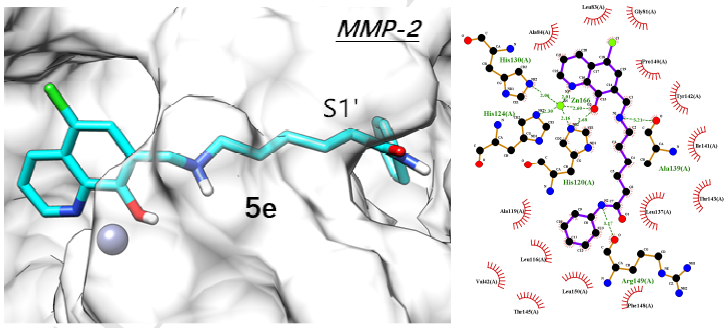

Fig. 4. Predicted binding mode of compound **5e** in MMP-2 enzyme (PDB: 1HOV).

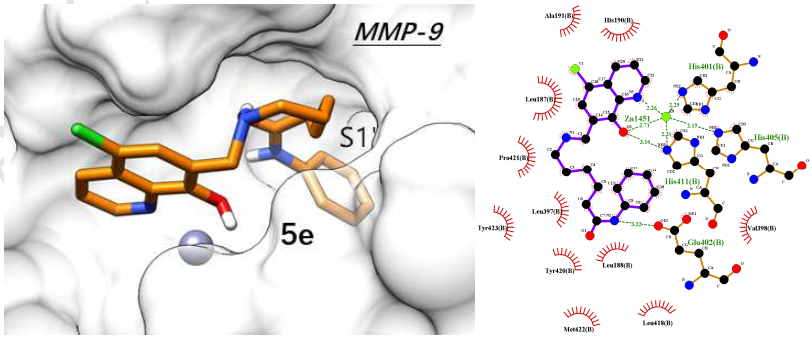

Fig. 5. Predicted binding mode of compound **5e** in MMP-9 enzyme (PDB: 1GKC).

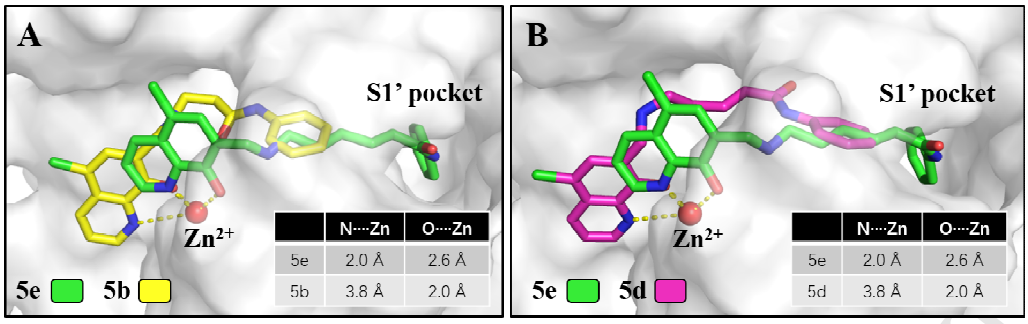

Fig. 6. (A) Comparison of the predicted binding modes of **5e** and **5b** in MMP-2. (B) Comparison of the predicted binding modes of **5e** and **5d** in MMP-2.

2.4. In vitro anti-proliferative assay

We further evaluated the anti-proliferative activities of **5a**, **5b**, **5d**, **5c**, **5d**, **5e**, **5h** and **5j**, which possessed good MMP-2/9 inhibitory activities, using MTT assays. All of these target compounds were screened against different cancer cell lines (HL-60, K562, KG1, A549, PC-3 and MCF-7) along with human umbilical vein endothelial cells (HUVECs). The IC_{50} values were summarized in Table 2. All compounds exhibited inhibitory activities against six cancer cell lines with comparable or slightly improved anti-proliferative activities when compared to known MMP-2 inhibitor compound **A**. Interestingly, hematologic tumor cells (K562 and KG1) seem to be more sensitive to our compounds than solid tumor cells (PC-3 and MCF-7). On the other hand, hydroxamate-based MMP inhibitors **NNGH** exerted 29-187 μM anti-proliferation activities for different cancer cell lines and **Prinomastat** possessed no cytotoxicity in these cancer cell lines.

Table. 2. Anti-proliferative activities of **5a**, **5b**, **5c**, **5d**, **5e**, **5h**, **5j, A, NNGH** and **Prinomastat**.

Compound	IC_{50}[a]（μM）						
	HL60	K562	KG1	A549	PC-3	MCF-7	HUVEC
5a	>5	2.9±0.03	2.3±0.43	7.4±0.37	10±0.95	13±0.03	>50
5b	1.3±0.09	1.7±0.20	1.1±0.07	9.7±0.55	1.9±0.10	13±1.7	>50
5c	1.9±0.04	1.9±0.05	1.6±0.11	17±0.31	7.7±0.06	9.0±1.0	>50
5d	1.9±0.19	2.9±0.04	1.6±0.10	13±0.24	8.4±0.18	7.4±0.64	>50
5e	1.8±0.11	2.3±0.07	2.3±0.09	11±0.14	8.3±0.10	4.6±0.14	>50
5h	4.0±0.57	1.8±0.08	0.69±0.09	6.4±0.69	22±0.29	7.8±0.63	>50
5j	2.6±0.12	4.2±0.69	4.7±0.02	>25	>25	12±0.61	>50
A	4.6±0.03	3.6±0.04	4.6±0.12	51±1.2	18±1.2	42±1.6	>50
NNGH	29±1.1	143±9.5	52±4.4	96±4.3	52±0.02	187±10	>250
Prinomastat	>500	>500	>500	>500	>500	>500	>500

[a] IC_{50} were expressed as the mean ± standard deviation of three separate determinations

2.5. Transwell migration and invasion assay

Since MMP-2 and MMP-9 were associated with increased tumor migration and invasion in lung cancer[24] and overexpression of MMP-2 and MMP-9 leads to poor prognosis in patients with NSCLC[25]. We further evaluated the effects of most active inhibitors (**5e** and **5h**) on tumor cell migration and invasion using A549 cell line (lung cancer).

The migration assay was performed using transwell chambers where fetal bovine serum (FBS)

acted as a chemoattractant. Briefly, A549 cells were incubated with compounds **5e**, **5h** and **A** for 24h. Then cells were seeded into the upper compartment of transwell chambers, whereas 10% FBS was used as chemoattractant and placed in the lower compartment. After 24h incubation, cells in the upper side of the filter were removed and cells that migrated to the lower surface were fixed, stained, captured and counted.

Results in **Fig. 7** showed that addition of 1, 5 and 10 μM of compounds **5e** and **5h** lead to an inhibition of A549 migration as compared to known inhibitor compound **A**. Compound **5e** display the strongest inhibitory effect on A549 cells migration in a dose dependent manner.

The invasion assay is similar with migration assay and the only difference is that transwell chambers are precoated with matrigel. Results in **Fig. 8** showed that compounds **5e** and **5h** have significant inhibitory effects on invasion of A549 cells as the concentration increases.

Furthermore, we compared anti-invasion activities of **5e**, **NNGH** and **Prinomastat**. Although compound **5e** exhibited weaker MMP inhibitory activities than **NNGH** and **Prinomastat** (**Table 1**), compound **5e** displayed similar anti-invasive activities to **NNGH** and better anti-invasive activities than **Prinomastat** (Supplementary material, Figure S2). The LogP values of **5e**, Prinomastat and NNGH have been calculated (Supplementary material, Table S3). The results found **5e** to possess higher LogP values than Prinomastat and NNGH, which may lead to better membrane permeability. This might be the reason that **5e** displayed similar or slightly better anti-invasive activities than reported inhibitors.

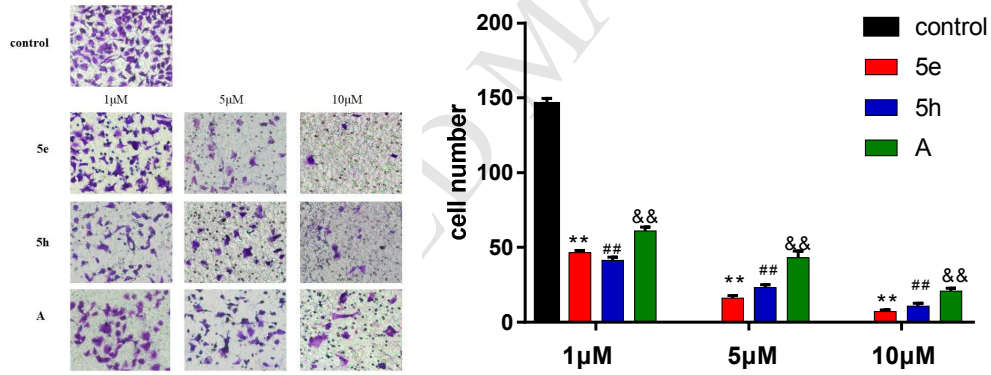

Fig. 7. Anti-migration activity of compounds against A549 cells at 1, 5 and 10 μM, imaging (left) and cell number (right) of migrated cells. All experiments were performed repeated three times. Means ± SEM are shown (** $p < 0.05$)

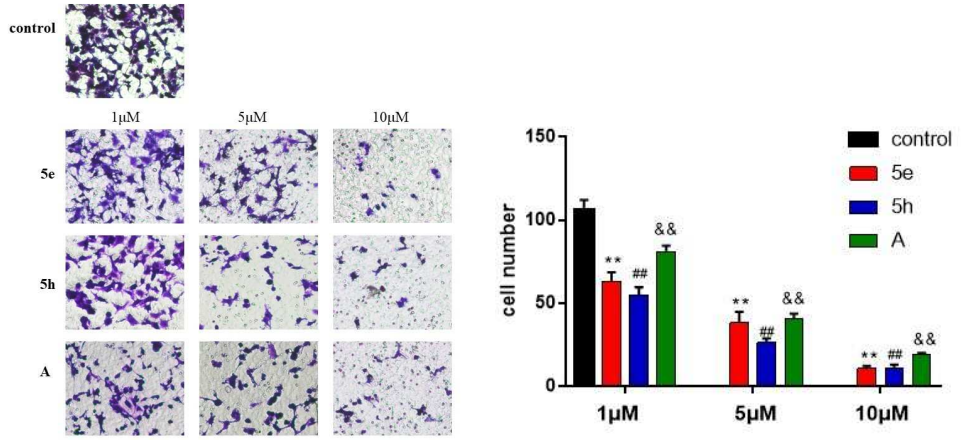

Fig. 8. Anti-invasion activity of compounds against A549 cells at 1, 5 and 10 μM, imaging (left) and cell number (right) of migrated cells. All experiments were performed repeated three times. Means ± SEM are shown (** $p < 0.05$)

2.6. HUVECs tuber formation assay

Since MMP-2 and MMP-9 are deeply involved in angiogenesis progression, we performed HUVECs tuber formation assay to examine whether compounds **5e** and **5h** could inhibit HUVECs tuber formation. According to **Table 2**, MTT assay indicated that **5e** and **5h** possess no cytotoxicity for HUVEC cells (IC_{50}> 50 μM). Then HUVECs tuber formation assay was performed *in vitro*. Results in **Fig. 9** showed that **5e** and **5h** significantly suppressed tube formation of HUVEC when compared with DMSO control. On the other hand, compound **A** exhibited moderate effects on tuber formation (**Fig. 9**).

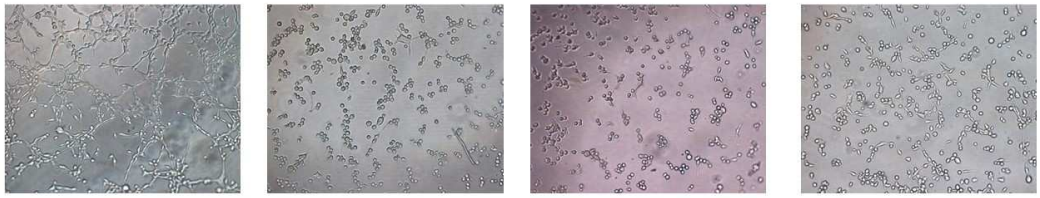

Fig. 9. HUVECs tuber formation assay of **5e**, **5h** and compound **A** at concentration of 10 μM.

2.7. Apoptotic assay

In order to evaluate whether compounds **5e** and **5h** could induce apoptosis in cancer cells, an Annexin-V/PI staining assay was conducted using A549 cells (**Fig. 10)**. Briefly, A549 cells were treated with **5e** and **5h** at the concentrations of 0, 1, 5 and 10 μM for 48 h. At the concentrations of 1 μM, compounds **5e** and **5h** could induce apoptosis with ratio of early apoptosis reaching 16%. As the concentration of **5h** increase, the percentage of early and late stage apoptotic cells increased to 38%. According to these results, we conclude that **5e** and **5h** can effectively induce apoptosis in A549 cells.

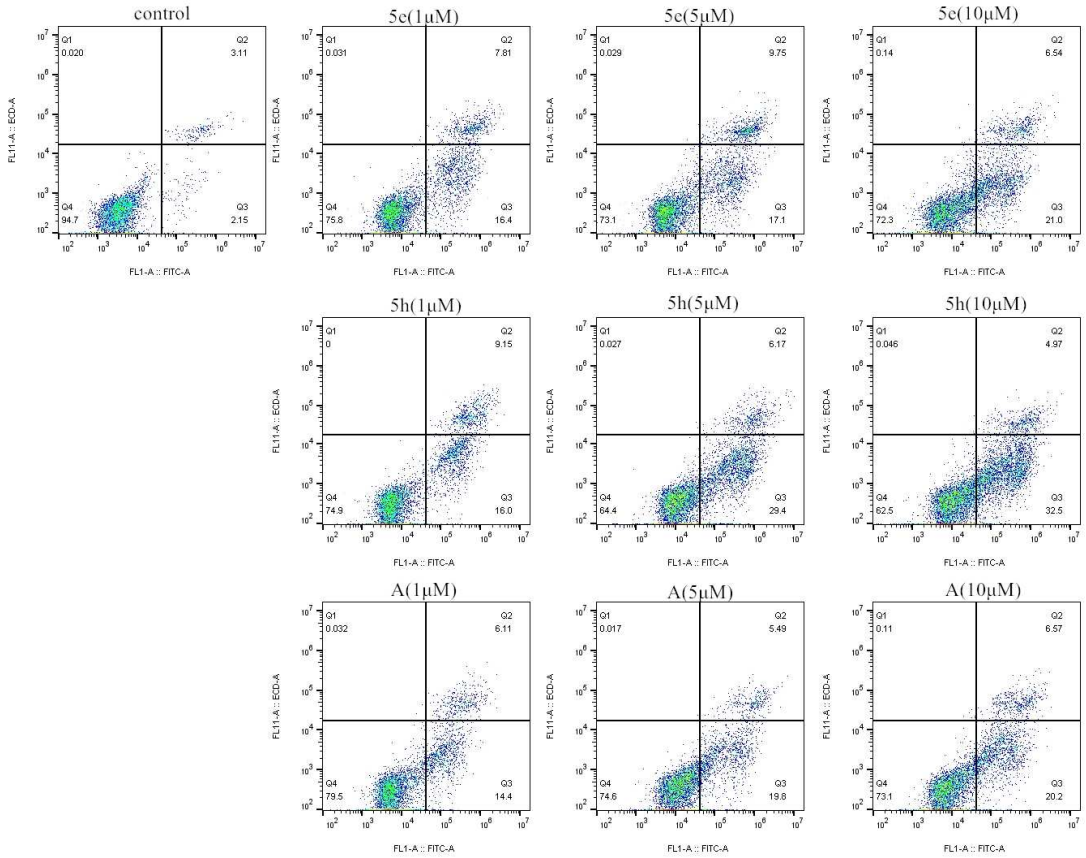

Fig. 10. Effects of **5e**, **5h** and **A** on apoptosis of A549 cells at 1 μM, 5 μM and 10 μM after 48 h.

2.7. Western blot and Gelatine zymography assay

In order to further investigate the MMPs inhibitory activities of our new inhibitors at the cellular level, western blot analysis was performed to measure the effects of **5e** and **5h** on MMP-2/9 expression using A549 cells. Results in **Fig. 11** indicated that **5e** and **5h** could markedly decrease expression levels of both MMP-2 and MMP-9 as the compound concentration increase.

Furthermore, gelatin zymography assay was performed to confirm the inhibitory activities of compound **5e** and **5h** on MMP-2 and MMP-9. As shown in **Fig. 12**, compound **5e** and **5h** significantly decreased the gelatinolytic activity of MMP-2 and MMP-9 in a dose dependent manner.

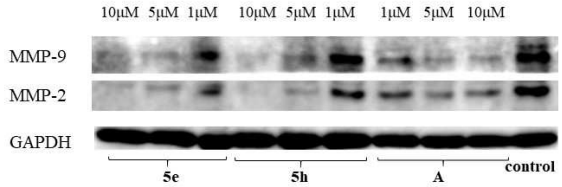

Fig. 11. Western blot analysis of MMP-2 and MMP-9 expressions in A549 cell after 24 h treatment with **5e**, **5h** at 1, 5 and 10 μM.

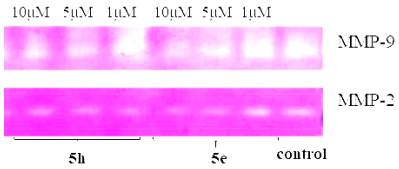

Fig. 12. Gelatine zymography analysis of MMP-2 and MMP-9 in A549 cell after 24 h treatment with **5e**, **5h** at 1, 5 and 10 μM.

3. Conclusions

In summary, a series of 8-hydroxyquinoline derivatives were designed and synthesized as new MMP-2/9 inhibitors. The most potent inhibitors **5e** and **5h** displayed anti-proliferation activities against several cancer cell lines and exhibited anti-migration/invasion activities on A549 cells. Moreover, HUVECs tuber formation assay was performed to measure the effects of compounds **5e** and **5h** on HUVEC angiogenesis. Our results indicated that compounds **5e** and **5h** possess good anti-invasion and anti-angiogenesis activity. Meanwhile, flow cytometry analysis showed that compound **5e** can promote A549 cell apoptosis *in vitro*. Furthermore, western blot analysis confirmed that both **5e** and **5h** could induce down-regulation of MMP-2 and MMP-9 expressions. Also, molecular docking studies not only revealed the favorable binding modes of **5e** with MMP-2/9, but also help us to understand the SAR of our new inhibitors. In the future, compound **5e** could serve as lead compound to develop more potent non-hydroxamate MMP-2/9 inhibitors.

4. Experimental

4.1. Chemistry

Reagents and solvents used were of commercially available LR grade quality and without further purification. All reactions were monitored by TLC on 0.25 mm silica gel plates (60 GF-254). UV light, chloride ferric and iodine vapor were used to visualize the spots. Melting points were recorded by the RY-1G electrothermal melting point apparatus without correction. ^{1}H and ^{13}C NMR spectra were recorded on a Brucker DRX spectrometer at 300 MHz or 400 MHz, *d* in parts per million and *J* in hertz, using TMS as an internal standard. Significant ^{1}H NMR data are reported in the following order: multiplicity (s, singlet; d, doublet; t, triplet; m, multiplet) number of protons. High-resolution mass spectra (HRMS) were conducted on an Agilent 6510 Quadrupole Time-of-Flight LC/MS deliver.

4.2. General synthesis of compounds

4.2.1. General procedure for the synthesis of 5a-5s

5-Chloro-8-hydroxyquinoline-7-carbaldehyde (0.21g, 1 mmol) and compound **4a-j** (1 mmol) was dissolved in MeOH (10ml) and reacted at RT for 4 h. Then $NaBH_4$ (3 equiv) was added to the reaction mixture, the solution was next stirred for 2h at RT. The MeOH was evaporated under reduced pressure and EtOAc was added. The EtOAc layer was washed with a saturated solution of

$NaHCO_3$ (×3), brine solution (×3) and then dried and evaporated. The crude product was purified by column chromatography (DCM/MeOH, 30/1-20/1) yielding target compounds **5a**-**5s**.

2-{[(5-chloro-8-hydroxyquinolin-7-yl)methyl]amino}-N-phenylacetamide (5a)

Yellow solid (Yield 32%), Mp:116-118℃. ^{1}H NMR (400 MHz, DMSO) δ 9.91 (s, 1H), 8.99 – 8.91 (m, 1H), 8.47 (dd, *J* = 8.5, 1.1 Hz, 1H), 7.77 (s, 1H), 7.69 (dd, *J* = 8.5, 4.1 Hz, 1H), 7.64 (d, *J* = 7.8 Hz, 2H), 7.30 (t, *J* = 7.9 Hz, 2H), 7.05 (t, *J* = 7.4 Hz, 1H), 3.97 (s, 2H), 3.35 (s, 2H). ^{13}C NMR (101 MHz, DMSO) δ 170.41, 151.23, 149.30, 139.23, 139.17, 132.83, 129.13, 128.77, 125.30, 123.69, 123.38, 122.99, 119.68, 118.43, 52.39, 47.72. HRMS (ESI) m/z Calcd $[M+H]^+$ 342.1004, found: 342.0981.

3-{[(5-chloro-8-hydroxyquinolin-7-yl)methyl]amino}-N-phenylpropanamide (5b)

Yellow solid (Yield 37%), Mp:120-122℃. ^{1}H NMR (400 MHz, $CDCl_3$) δ 9.96 (s, 1H), 8.85 (dd, *J* = 4.1, 1.3 Hz, 1H), 8.51 (dd, *J* = 8.5, 1.4 Hz, 1H), 7.57 – 7.48 (m, 4H), 7.34 – 7.27 (m, 2H), 7.07 (t, *J* = 7.4 Hz, 1H), 4.12 (s, 2H), 3.05 (t, 2H), 2.57 (t, 2H). ^{13}C NMR (101 MHz, DMSO) δ 170.62, 151.82, 149.33, 139.68, 139.37, 132.78, 129.07, 128.53, 125.33, 123.48, 122.95, 122.69, 119.60, 118.15, 47.93, 44.98, 36.80. HRMS (ESI) m/z Calcd $[M+H]^+$ 356.1060, found: 356.1145.

4-{[(5-chloro-8-hydroxyquinolin-7-yl)methyl]amino}-N-phenylbutanamide (5c)

Yellow solid (Yield 27%), Mp:78-80℃. ^{1}H NMR (400 MHz, $CDCl_3$) δ 8.84 (d, *J* = 3.2 Hz, 1H), 8.47 (d, *J* = 8.5 Hz, 1H), 7.49 (dd, *J* = 8.5, 4.1 Hz, 1H), 7.44 (d, *J* = 7.9 Hz, 2H), 7.37 (s, 1H), 7.25 – 7.20 (m, 2H), 7.04 (t, 1H), 4.10 (s, 2H), 2.81 (t, *J* = 6.0 Hz, 2H), 2.51 (t, *J* = 6.8 Hz, 2H), 2.01 – 1.90 (m, 2H). ^{13}C NMR (101 MHz, DMSO) δ 170.41, 151.23, 149.30, 139.23, 139.17, 132.83, 129.13, 128.77, 125.30, 123.69, 123.38, 122.99, 119.68, 118.43, 52.39, 47.72. HRMS (ESI) m/z Calcd $[M+H]^+$ 370.1319, found: 370.1299.

5-{[(5-chloro-8-hydroxyquinolin-7-yl)methyl]amino}-N-phenylpentanamide (5d)

Yellow solid (Yield 34%), Mp:102-105℃. ^{1}H NMR (400 MHz, $CDCl_3$) δ 8.82 (d, *J* = 3.1 Hz, 1H), 8.47 (dd, *J* = 8.5, 1.3 Hz, 1H), 8.06 (s, 1H), 7.62 (d, *J* = 7.9 Hz, 1H), 7.48 (dd, *J* = 8.5, 4.1 Hz, 1H), 7.35 (s, 1H), 7.29 (t, *J* = 7.8 Hz, 2H), 7.08 (t, *J* = 7.3 Hz, 2H), 4.13 (s, 2H), 2.73 (t, *J* = 6.5 Hz, 2H), 2.34 – 2.26 (m, 2H), 1.88 – 1.79 (m, 2H), 1.69 – 1.61 (m, 2H). ^{13}C NMR (101 MHz, DMSO) δ 170.41, 151.23, 149.30, 139.23, 139.17, 132.83, 129.13, 128.77, 125.30, 123.69, 123.38, 122.99, 119.68, 118.43, 52.39, 47.72. HRMS (ESI) m/z Calcd $[M+H]^+$ 384.1473, found: 384.1456.

6-{[(5-chloro-8-hydroxyquinolin-7-yl)methyl]amino}-N-phenylhexanamide (5e)

Yellow solid (Yield 24%), Mp:116-118℃. ^{1}H NMR (400 MHz, DMSO) δ 9.86 (s, 1H), 8.91 (d, *J* = 2.9 Hz, 1H), 8.45 (d, *J* = 8.5 Hz, 1H), 7.71 – 7.62 (m, 2H), 7.58 (d, *J* = 7.9 Hz, 2H), 7.27 (t, *J* = 7.8 Hz, 2H), 7.02 (d, *J* = 7.3 Hz, 1H), 3.96 (s, 2H), 2.54 (t, *J* = 6.9 Hz, 2H), 2.30 (t, *J* = 7.4 Hz, 2H), 1.64 – 1.55 (m, 2H), 1.53 – 1.45 (m, 2H), 1.38 – 1.32 (m, 2H). ^{13}C NMR (101 MHz, DMSO) δ 170.41, 151.23, 149.30, 139.23, 139.17, 132.83, 129.13, 128.77, 125.30, 123.69, 123.38, 122.99, 119.68, 118.43, 52.39, 47.72. HRMS (ESI) m/z Calcd $[M+H]^+$ 398.1629, found: 398.1611.

2-{[(5-chloro-8-hydroxyquinolin-7-yl)methyl]amino}-N-[2-(2-methyl-1H-indol-3-yl)ethyl]acet

amide (5f)

Yellow solid (Yield 42%), Mp:113-116□. ^{1}H NMR (400 MHz, DMSO) δ 10.69 (s, 1H), 8.94 (dd, *J* = 4.1, 1.4 Hz, 1H), 8.48 (dd, *J* = 8.5, 1.3 Hz, 1H), 7.97 (t, *J* = 5.8 Hz, 1H), 7.73 – 7.66 (m, 2H), 7.43 (d, *J* = 7.6 Hz, 1H), 7.21 (d, *J* = 7.8 Hz, 1H), 6.95 (t, *J* = 10.9, 4.0 Hz, 1H), 6.91 (t, *J* = 10.8, 3.9 Hz, 1H), 3.86 (s, 2H), 3.25 (dd, *J* = 14.2, 6.6 Hz, 2H), 3.11 (s, 2H), 2.76 (t, *J* = 7.5 Hz, 2H), 2.31 (s, 3H). ^{13}C NMR (101 MHz, $CDCl_3$) δ 171.28, 149.35, 148.66, 138.50, 135.32, 133.24, 131.91, 128.65, 128.41, 125.54, 122.33, 121.10, 121.06, 120.09, 119.28, 117.83, 110.40, 108.53, 77.38, 77.26, 77.06, 76.74, 51.78, 48.61, 39.45, 24.14, 11.65. HRMS (ESI) m/z Calcd $[M+H]^+$ 423.1582, found: 423.1547.

3-{[(5-chloro-8-hydroxyquinolin-7-yl)methyl]amino}-N-[2-(2-methyl-1H-indol-3-yl)ethyl]propanamide (5g)

Yellow solid (Yield 22%), Mp:120-122□. ^{1}H NMR (400 MHz, $CDCl_3$) δ 8.78 (s, 1H), 8.34 (d, *J* = 8.2 Hz, 1H), 7.96 (d, *J* = 21.2 Hz, 2H), 7.50 (dd, *J* = 8.3, 4.2 Hz, 1H), 7.36 (d, *J* = 7.6 Hz, 1H), 7.18 (d, *J* = 7.7 Hz, 2H), 7.03 (dt, *J* = 14.5, 6.9 Hz, 2H), 6.13 (s, 1H), 3.90 (s, 2H), 3.45 (dd, *J* = 12.5, 6.3 Hz, 2H), 2.82 (t, *J* = 6.6 Hz, 2H), 2.55 (t, 2H), 2.21 (s, 3H), 1.69 (t, 2H). ^{13}C NMR (101 MHz, $CDCl_3$) δ 171.28, 149.35, 148.66, 138.50, 135.32, 133.24, 131.91, 128.65, 128.41, 125.54, 122.33, 121.10, 121.06, 120.09, 119.28, 117.83, 110.40, 108.53, 77.38, 77.26, 77.06, 76.74, 51.78, 48.61, 39.45, 24.14, 11.65. HRMS (ESI) m/z Calcd $[M+H]^+$ 437.1638, found: 437.1551.

4-{[(5-chloro-8-hydroxyquinolin-7-yl)methyl]amino}-N-[2-(2-methyl-1H-indol-3-yl)ethyl]butanamide (5h)

Yellow solid (Yield 39%), Mp:115-117□. ^{1}H NMR (400 MHz, $CDCl_3$) δ 8.87 (dd, *J* = 4.2, 1.5 Hz, 1H), 8.47 (dd, *J* = 8.5, 1.6 Hz, 1H), 7.91 (s, 1H), 7.49 (dd, *J* = 8.6, 4.2 Hz, 1H), 7.46 (d, *J* = 7.4 Hz, 1H), 7.34 (s, 1H), 7.24 (s, 1H), 7.12 – 7.07 (m, 1H), 7.07 – 7.02 (m, 1H), 4.03 (s, 2H), 3.44 (d, *J* = 6.2 Hz, 2H), 2.86 (t, *J* = 6.8 Hz, 2H), 2.65 (t, *J* = 6.7 Hz, 2H), 2.34 (s, 3H), 2.19 (t, *J* = 7.2 Hz, 2H), 1.85 – 1.80 (m, 2H). ^{13}C NMR (101 MHz, $CDCl_3$) δ 171.28, 149.35, 148.66, 138.50, 135.32, 133.24, 131.91, 128.65, 128.41, 125.54, 122.33, 121.10, 121.06, 120.09, 119.28, 117.83, 110.40, 108.53, 77.38, 77.26, 77.06, 76.74, 51.78, 48.61, 39.45, 24.14, 11.65. HRMS (ESI) m/z Calcd $[M+H]^+$ 451.1895, found: 451.1872.

5-{[(5-chloro-8-hydroxyquinolin-7-yl)methyl]amino}-N-[2-(2-methyl-1H-indol-3-yl)ethyl]pentanamide (5i)

Yellow solid (Yield 25%), Mp:104-106□. ^{1}H NMR (400 MHz, $CDCl_3$) δ 8.90 (dd, *J* = 4.1, 1.5 Hz, 1H), 8.75 (s, 1H), 8.49 (dd, *J* = 8.5, 1.5 Hz, 1H), 7.53 – 7.46 (m, 2H), 7.33 (s, 1H), 7.25 – 7.21 (m, 1H), 7.11 – 7.02 (m, 2H), 4.07 (s, 2H), 3.52 (dd, *J* = 12.6, 6.4 Hz, 2H), 2.92 (t, *J* = 6.6 Hz, 2H), 2.65 (t, *J* = 6.6 Hz, 2H), 2.37 (s, 3H), 2.07 (dd, *J* = 13.2, 5.5 Hz, 2H), 1.66 – 1.54 (m, 2H), 1.55 – 1.45 (m, 2H). ^{13}C NMR (101 MHz, $CDCl_3$) δ 171.28, 149.35, 148.66, 138.50, 135.32, 133.24, 131.91, 128.65, 128.41, 125.54, 122.33, 121.10, 121.06, 120.09, 119.28, 117.83, 110.40, 108.53, 77.38, 77.26, 77.06, 76.74, 51.78, 48.61, 39.45, 24.14, 11.65. HRMS (ESI) m/z Calcd $[M+H]^+$ 465.2051, found: 465.2023.

6-{[(5-chloro-8-hydroxyquinolin-7-yl)methyl]amino}-N-[2-(2-methyl-1H-indol-3-yl)ethyl]hexanamide (5j)

Yellow solid (Yield 32%), Mp:98-101℃. ^{1}H NMR (400 MHz, $CDCl_3$) δ 8.87 (d, *J* = 2.8 Hz, 1H), 8.47 (dd, *J* = 8.5, 1.4 Hz, 1H), 7.52 – 7.44 (m, 2H), 7.35 (s, 1H), 7.29 – 7.24 (m, 2H), 7.19 – 6.99 (m, 3H), 4.09 (s, 2H), 3.54 – 3.45 (m, 2H), 2.89 (t, *J* = 6.6 Hz, 2H), 2.65 (t, *J* = 7.0 Hz, 2H), 2.34 (s, 3H), 2.08 – 2.04 (m, 2H), 1.61 – 1.46 (m, 4H), 1.29 – 1.23 (m, 2H). ^{13}C NMR (101 MHz, $CDCl_3$) δ 171.28, 149.35, 148.66, 138.50, 135.32, 133.24, 131.91, 128.65, 128.41, 125.54, 122.33, 121.10, 121.06, 120.09, 119.28, 117.83, 110.40, 108.53, 77.38, 77.26, 77.06, 76.74, 51.78, 48.61, 39.45, 24.14, 11.65. HRMS (ESI) m/z Calcd $[M+H]^+$ 479.2208, found: 479.2194.

2-{[(8-hydroxyquinolin-5-yl)methyl]amino}-N-phenylacetamide (5k)

Yellow solid (Yield 33%), Mp:115-118□. ^{1}H NMR (400 MHz, $CDCl_3$) δ 9.00 (s, 1H), 8.82 (dd, *J* = 4.1, 1.2 Hz, 1H), 8.49 (dd, *J* = 8.5, 1.2 Hz, 1H), 7.52 (dd, *J* = 8.5, 4.2 Hz, 1H), 7.45 – 7.37 (m, 3H), 7.29 (t, *J* = 8.0 Hz, 1H), 7.12 (d, *J* = 7.7 Hz, 1H), 7.08 (t, *J* = 7.4 Hz, 1H), 4.21 (s, 2H), 3.50 (s, 2H). ^{13}C NMR (101 MHz, $CDCl_3$) δ 169.48, 152.21, 147.73, 138.84, 137.44, 132.37, 129.00, 128.51, 126.96, 125.07, 124.17, 122.00, 119.17, 109.16, 52.73, 51.03. HRMS (ESI) m/z Calcd $[M+H]^+$ 308.1393, found: 308.1378.

3-{[(8-hydroxyquinolin-5-yl)methyl]amino}-N-phenylpropanamide (5l)

Yellow solid (Yield 39%), Mp:121-124□.^{1}H NMR (400 MHz, $CDCl_3$) δ 9.96 (s, 1H), 8.80 (dd, *J* = 4.2, 1.4 Hz, 1H), 8.46 (dd, *J* = 8.5, 1.4 Hz, 1H), 7.44 (d, *J* = 7.4 Hz, 1H), 7.42 – 7.39 (m, 1H), 7.35 – 7.28 (m, 2H), 7.24 (t, 2H), 7.13 (d, *J* = 7.7 Hz, 1H), 7.05 (t, *J* = 7.3 Hz, 1H), 4.20 (s, 2H), 3.12 (t, 2H), 2.56 (t, 2H). ^{13}C NMR (101 MHz, DMSO) δ 171.02, 152.93, 148.10, 139.70, 139.25, 133.91, 129.11, 128.01, 127.84, 127.04, 123.44, 121.82, 119.49, 110.56, 50.55, 45.76, 37.35. HRMS (ESI) m/z Calcd $[M+H]^+$ 322.1550, found: 322.1522.

4-{[(8-hydroxyquinolin-5-yl)methyl]amino}-N-phenylbutanamide(5m)

Yellow solid (Yield 34%), Mp:140-143□. ^{1}H NMR (400 MHz, $CDCl_3$) δ 8.75 (dd, *J* = 4.2, 1.5 Hz, 1H), 8.47 (dd, *J* = 8.5, 1.5 Hz, 1H), 8.16 (s, 1H), 7.43 – 7.40 (m, 1H), 7.39 (d, *J* = 2.8 Hz, 1H), 7.34 (d, *J* = 7.8 Hz, 2H), 7.23 (d, *J* = 8.2 Hz, 2H), 7.08 (d, *J* = 7.7 Hz, 1H), 7.05 (d, *J* = 7.3 Hz, 1H), 4.14 (s, 2H), 2.85 (t, *J* = 6.4 Hz, 2H), 2.46 (t, *J* = 6.9 Hz, 2H), 1.98 – 1.88 (m, 2H). ^{13}C NMR (101 MHz, $CDCl_3$) δ 171.61, 151.66, 147.50, 138.70, 138.64, 133.19, 128.65, 127.73, 127.24, 126.54, 123.50, 121.61, 119.65, 108.97, 77.58, 77.46, 77.26, 76.94, 50.90, 49.06, 40.47, 40.26, 40.05, 39.85, 39.64, 39.42, 35.35, 25.62. HRMS (ESI) m/z Calcd $[M+H]^+$ 336.1706, found: 336.1687.

5-{[(8-hydroxyquinolin-5-yl)methyl]amino}-N-phenylpentanamide (5n)

Yellow solid (Yield 31%), Mp:122-124□. ^{1}H NMR (400 MHz, $CDCl_3$) δ 8.77 (d, *J* = 3.1 Hz, 1H), 8.55 – 8.47 (m, 1H), 7.48 – 7.36 (m, 4H), 7.29 (d, *J* = 7.6 Hz, 2H), 7.09 (d, *J* = 7.6 Hz, 2H), 4.11 (s, 2H), 2.76 (t, *J* = 6.8 Hz, 2H), 2.35 (t, *J* = 7.2 Hz, 2H), 1.83 – 1.76 (m, 2H), 1.64 – 1.56 (m, 2H). ^{13}C NMR (101 MHz, DMSO) δ 171.72, 152.78, 148.07, 139.84, 139.23, 133.84, 129.09, 127.84, 127.79, 127.32, 123.36, 121.81, 119.49, 110.51, 50.80, 49.30, 36.82, 29.57, 23.53. HRMS (ESI) m/z Calcd $[M+H]^+$ 350.1863, found: 350.1863.

6-{[(8-hydroxyquinolin-5-yl)methyl]amino}-N-phenylhexanamide (5o)

Yellow solid (Yield 28%), Mp:125-128□. ^{1}H NMR (400 MHz, $CDCl_3$) δ 8.80 – 8.74 (m, 1H), 8.52 (d, 1H), 7.49 (d, *J* = 9.1 Hz, 2H), 7.47 – 7.44 (m, 1H), 7.38 (d, *J* = 7.8 Hz, 1H), 7.31 (t, *J* = 7.8 Hz, 2H), 7.08 (d, *J* = 7.7 Hz, 2H), 4.11 (s, 2H), 2.72 (t, *J* = 7.1 Hz, 2H), 2.34 (t, *J* = 7.4 Hz, 2H), 1.76 – 1.71 (m, 2H), 1.59 – 1.55 (m, 2H), 1.45 – 1.39 (m, 2H). ^{13}C NMR (101 MHz, DMSO) δ 171.72, 152.81, 148.05, 139.85, 139.24, 133.83, 129.08, 127.84, 127.78, 127.32, 123.35, 121.78, 119.49, 110.52, 50.82, 49.47, 36.91, 29.73, 27.06, 25.59. HRMS (ESI) m/z Calcd $[M+H]^+$ 364.2019, found: 364.2005.

7-{[(8-hydroxyquinolin-5-yl)methyl]amino}-N-phenylheptanamide (5p)

Yellow solid (Yield 31%), Mp:96-98℃. ^{1}H NMR (400 MHz, $CDCl_3$) δ 8.78 (d, *J* = 3.0 Hz, 1H), 8.52 (d, *J* = 8.5 Hz, 1H), 7.54 – 7.46 (m, 3H), 7.40 (d, *J* = 7.7 Hz, 1H), 7.31 (t, *J* = 7.7 Hz, 2H), 7.17 (d, *J* = 8.0 Hz, 1H), 7.10 (t, *J* = 6.8 Hz, 2H), 4.12 (s, 2H), 2.70 (t, *J* = 7.1 Hz, 2H), 2.32 (t, *J* = 7.5 Hz, 2H), 1.74 (d, *J* = 26.9 Hz, 2H), 1.51 (d, *J* = 26.9 Hz, 2H), 1.42 – 1.30 (m, 4H). ^{13}C NMR (101 MHz, DMSO) δ 171.72, 152.79, 148.06, 139.84, 139.22, 133.84, 129.09, 127.84, 127.80, 127.32, 123.35, 121.79, 119.47, 110.51, 50.83, 49.54, 36.87, 29.84, 29.13, 27.16, 25.63. HRMS (ESI) m/z Calcd $[M+H]^+$ 378.2176, found: 378.2162.

3-{[(8-hydroxyquinolin-5-yl)methyl]amino}-N-[2-(2-methyl-1H-indol-3-yl)ethyl]propanamide(5q)

Yellow solid (Yield 36%), Mp:92-94□. ^{1}H NMR (400 MHz, $CDCl_3$) δ 8.74 (dd, *J* = 4.2, 1.4 Hz, 1H), 8.19 (dd, *J* = 8.5, 1.4 Hz, 1H), 7.61 (s, 1H), 7.43 – 7.38 (m, 1H), 7.32 – 7.29 (m, 1H), 7.18 (d, *J* = 7.7 Hz, 1H), 7.14 – 7.10 (m, 1H), 7.04 (ddd, *J* = 6.5, 3.7, 1.9 Hz, 3H), 3.88 (s, 2H), 3.41 (dd, *J* = 12.8, 6.5 Hz, 2H), 2.87 – 2.78 (m, 4H), 2.35 – 2.29 (m, 2H), 2.27 (d, *J* = 6.3 Hz, 3H). ^{13}C NMR (101 MHz, DMSO) δ 171.74, 153.33, 152.93, 148.11, 139.25, 135.65, 133.83, 132.51, 128.78, 127.83, 126.90, 121.83, 120.36, 118.54, 117.76, 110.82, 110.55, 108.09, 55.87, 50.47, 45.82, 36.20, 24.70, 11.67. HRMS (ESI) m/z Calcd $[M+H]^+$ 403.2128, found: 403.2090.

4-{[(8-hydroxyquinolin-5-yl)methyl]amino}-N-[2-(2-methyl-1H-indol-3-yl)ethyl]butanamide (5r)

Yellow solid (Yield 27%), Mp:95-98□. ^{1}H NMR (400 MHz, $CDCl_3$) δ 8.76 (dd, *J* = 4.2, 1.4 Hz, 1H), 8.44 (dd, *J* = 8.5, 1.5 Hz, 1H), 7.46 (d, *J* = 7.4 Hz, 1H), 7.44 (d, *J* = 4.1 Hz, 1H), 7.42 (d, *J* = 4.2 Hz, 1H), 7.32 (d, *J* = 7.7 Hz, 1H), 7.23 (d, 1H), 7.12 (d, 1H), 7.08 (d, *J* = 3.2 Hz, 1H), 7.07 – 7.05 (m, 1H), 4.00 (s, 2H), 3.45 (dd, *J* = 12.8, 6.6 Hz, 2H), 2.86 (t, *J* = 6.7 Hz, 2H), 2.65 (t, *J* = 6.7 Hz, 2H), 2.31 (s, 3H), 2.17 (t, *J* = 7.2 Hz, 2H), 1.78 (t, 2H). ^{13}C NMR (101 MHz, DMSO) δ 172.66, 153.16, 152.92, 148.22, 139.13, 135.63, 133.71, 132.54, 128.77, 128.24, 127.79, 125.35, 121.95, 120.39, 118.58, 117.75, 110.84, 110.58, 108.07, 50.06, 48.83, 33.87, 25.56, 24.62, 11.61. HRMS (ESI) m/z Calcd $[M+H]^+$ 417.2285, found: 417.2270.

5-{[(8-hydroxyquinolin-5-yl)methyl]amino}-N-[2-(2-methyl-1H-indol-3-yl)ethyl]pentanamide (5s)

Yellow solid (Yield 33%), Mp:134-136□. ^{1}H NMR (400 MHz, $CDCl_3$) δ 8.77 (dd, *J* = 4.2, 1.5 Hz, 1H), 8.50 (dd, *J* = 8.5, 1.5 Hz, 1H), 7.87 (s, 1H), 7.49 – 7.44 (m, 2H), 7.39 (d, *J* = 7.7 Hz, 1H), 7.13 – 7.02 (m, 4H), 4.08 (s, 2H), 3.50 – 3.44 (m, 2H), 2.88 (t, *J* = 8.7, 4.6 Hz, 2H), 2.66 (t, *J* =

6.9 Hz, 2H), 2.34 (s, 3H), 2.06 (t, *J* = 11.8, 4.3 Hz, 2H), 1.65 – 1.55 (m, 2H), 1.53 – 1.45 (m, 2H). ^{13}C NMR (101 MHz, $CDCl_3$) δ 172.85, 151.78, 147.57, 138.63, 135.32, 134.15, 133.20, 131.99, 129.57, 128.62, 127.64, 127.24, 125.54, 121.14, 119.33, 117.75, 110.39, 108.80, 50.86, 49.19, 39.90, 36.41, 29.34, 25.77, 24.15, 11.60. HRMS (ESI) m/z Calcd $[M+H]^+$ 431.2441, found: 431.2403.

4.2.2. General procedure for the synthesis of 10a-10l

Compound **9a-l** (1.2 mmol, 1.2 equiv) was dissolved in 20 mL DCM and one drop DMF was added. Then oxalyl chloride (0.2 mL, 2.4 mmol, 2.4 equiv) was added dropwise and the reaction was stirred at RT for 1h. After the mixture was evaropated, the residue was dissolved in DCM and again concentrated in vacuo to offer quantitatively the crude chloride. A solution of chloride in DCM (10 mL) was suspended with NEt_3 (0.3g, 3 equiv) and compound **7** (0.27g, 1mmol) was added dropwise with stirring. After the addition, the reaction was stirred for 4 h. Then the mixture was washed with 1M citric acid(×3), saturate solution of $NaHCO_3$(×3) and brine solution(×3). The solution was concentrated in vacuo, then purified via chlomatography on silica (PE/EA =3:1) to get **10a-l** as a white solid.

N-{8-[(tert-butyldimethylsilyl)oxy]quinolin-5-yl}-3-[methyl(phenyl)amino]propanamide(10a)

White solid (Yield 57%), Mp:149-151□.^{1}H NMR (400 MHz, $CDCl_3$) δ 8.77 (dd, *J* = 4.0, 1.4 Hz, 1H), 8.20 (s, 1H), 7.87 (dd, *J* = 8.5, 1.4 Hz, 1H), 7.46 (d, *J* = 8.2 Hz, 1H), 7.27 (d, *J* = 8.6 Hz, 2H), 7.18 (dd, *J* = 8.5, 4.0 Hz, 1H), 7.06 (d, *J* = 8.2 Hz, 1H), 6.80 (dd, *J* = 16.1, 7.9 Hz, 3H), 3.68 (t, *J* = 6.4 Hz, 2H), 2.93 (s, 3H), 2.66 – 2.58 (m, 2H), 1.05 (s, 9H), 0.24 (s, 6H).

N-{8-[(tert-butyldimethylsilyl)oxy]quinolin-5-yl}-4-[methyl(phenyl)amino]butanamide (10b)

White solid (Yield 66%), Mp:144-146□. ^{1}H NMR (400 MHz, $CDCl_3$) δ 8.80 (d, *J* = 2.9 Hz, 1H), 7.95 (d, *J* = 7.7 Hz, 1H), 7.53 (s, 1H), 7.40 (d, *J* = 8.2 Hz, 1H), 7.30 – 7.18 (m, 4H), 7.08 (d, *J* = 8.2 Hz, 1H), 6.74 (d, *J* = 8.2 Hz, 2H), 6.69 (t, *J* = 7.3 Hz, 1H), 3.39 (t, *J* = 7.0 Hz, 2H), 2.90 (s, 3H), 2.44 (t, *J* = 7.1 Hz, 2H), 2.00 (dd, *J* = 14.1, 7.0 Hz, 2H), 1.06 (s, 9H), 0.25 (s, 6H).

N-{8-[(tert-butyldimethylsilyl)oxy]quinolin-5-yl}-5-[methyl(phenyl)amino]pentanamide(10c)

Colourless oil (Yield 69%). ^{1}H NMR (400 MHz, $CDCl_3$) δ 8.85 (d, *J* = 3.0 Hz, 1H), 8.07 – 7.97 (m, 1H), 7.49 (d, *J* = 8.1 Hz, 1H), 7.36 (dd, *J* = 8.4, 3.9 Hz, 1H), 7.22 (d, *J* = 8.1 Hz, 2H), 7.13 (d, *J* = 8.2 Hz, 1H), 6.76 – 6.65 (m, 3H), 3.40 (s, 2H), 2.95 (s, 3H), 2.49 (t, *J* = 7.2 Hz, 2H), 1.88 – 1.79 (m, 2H), 1.77 – 1.70 (m, 2H), 1.06 (s, 9H), 0.26 (s, 6H).

N-{8-[(tert-butyldimethylsilyl)oxy]quinolin-5-yl}-6-[methyl(phenyl)amino]hexanamide (10d)

Colourless oil oil (Yield 61%). ^{1}H NMR (400 MHz, $CDCl_3$) δ 8.84 (t, *J* = 15.7 Hz, 1H), 8.00 (d, *J* = 8.5 Hz, 1H), 7.41 (dd, *J* = 7.6, 2.6 Hz, 1H), 7.34 – 7.24 (m, 1H), 7.20 (d, *J* = 7.6 Hz, 2H), 7.07 (d, *J* = 8.2 Hz, 1H), 6.67 (dd, *J* = 11.3, 7.9 Hz, 3H), 3.30 (dd, *J* = 8.9, 5.5 Hz, 2H), 2.89 (d, *J* = 4.9 Hz, 3H), 2.36 (t, *J* = 7.7 Hz, 2H), 1.74 (s, 2H), 1.59 (d, *J* = 7.5 Hz, 2H), 1.43 – 1.35 (m, 2H), 1.06 (s, 9H), 0.25 (s, 6H).

N-{8-[(tert-butyldimethylsilyl)oxy]quinolin-5-yl}-3-(2-methyl-1H-benzo[d]imidazol-1-yl)propanamide (10e)

Colourless oil (Yield 41%). ^{1}H NMR (400 MHz, $CDCl_3$). ^{1}H NMR (400 MHz, DMSO) δ 9.84 (s, 1H), 8.83 (dd, *J* = 4.0, 1.3 Hz, 1H), 7.84 (dd, *J* = 8.6, 1.3 Hz, 1H), 7.55 (dd, *J* = 10.0, 3.8 Hz, 2H), 7.38 (dd, *J* = 8.6, 4.1 Hz, 1H), 7.35 (d, *J* = 8.2 Hz, 1H), 7.20 – 7.14 (m, 2H), 7.13 (d, *J* = 8.2 Hz, 1H), 4.54 (s, 2H), 2.97 (s, 2H), 2.59 (s, 3H), 1.01 (s, 9H), 0.20 (s, 6H).

N-{8-[(tert-butyldimethylsilyl)oxy]quinolin-5-yl}-4-(2-methyl-1H-benzo[d]imidazol-1-yl)butanamide (10f)

White solid (Yield 49%), Mp:133-135□. ^{1}H NMR (400 MHz, DMSO) δ 9.79 (s, 1H), 8.81 (dd, *J* = 4.0, 1.4 Hz, 1H), 8.10 (dd, *J* = 8.6, 1.4 Hz, 1H), 7.40– 7.30 (m, 4H), 7.10 – 7.00 (m, 3H), 4.15 (t, *J* = 7.0 Hz, 2H), 2.46 (s, 3H), 2.35 – 2.30 (m, 2H), 1.72 – 1.69 (m, 2H), 0.93 (s, 9H), 0.18 (s, 6H).

N-{8-[(tert-butyldimethylsilyl)oxy]quinolin-5-yl}-5-(2-methyl-1H-benzo[d]imidazol-1-yl)pentanamide (10g)

White solid (Yield 52%), Mp:142-144□. ^{1}H NMR (400 MHz, DMSO) δ 9.74 (s, 1H), 8.79 (dd, *J* = 4.0, 1.4 Hz, 1H), 8.18 (dd, *J* = 8.6, 1.4 Hz, 1H), 7.46 – 7.35 (m, 4H), 7.10 – 7.00 (m, 3H), 4.15 (t, *J* = 7.0 Hz, 2H), 2.46 (s, 3H), 2.42 – 2.39 (m, 2H), 1.77 – 1.68 (m, 2H), 1.65 – 1.54 (m, 2H), 0.93 (s, 9H), 0.13 (s, 6H).

N-{8-[(tert-butyldimethylsilyl)oxy]quinolin-5-yl}-6-(2-methyl-1H-benzo[d]imidazol-1-yl)hexanamide (10h)

White solid (Yield 53%), Mp:132-134□. ^{1}H NMR (400 MHz, DMSO) δ 9.76 (s, 1H), 8.87 (dd, *J* = 4.0, 1.3 Hz, 1H), 8.27 (dd, *J* = 8.6, 1.4 Hz, 1H), 7.56 – 7.42 (m, 4H), 7.18 – 7.10 (m, 3H), 4.20 (t, *J* = 7.1 Hz, 2H), 2.54 (s, 3H), 2.41 (t, *J* = 7.1 Hz, 2H), 1.81 – 1.73 (m, 2H), 1.71 – 1.64 (m, 2H), 1.42 – 1.35 (m, 2H), 1.02 (s, 9H), 0.21 (s, 6H).

N-{8-[(tert-butyldimethylsilyl)oxy]quinolin-5-yl}-3-{1,1-dioxido-3-oxobenzo[d]isothiazol-2(3H)-yl}propanamide (10i)

White solid (Yield 63%), Mp:102-104□.^{1}H NMR (400 MHz, $CDCl_3$) δ 8.83 (dd, *J* = 4.0, 1.3 Hz, 1H), 8.09 (dd, *J* = 11.2, 4.1 Hz, 2H), 7.99 – 7.80 (m, 3H), 7.56 (d, *J* = 8.2 Hz, 1H), 7.47 (s, 1H), 7.33 (dd, *J* = 8.5, 4.1 Hz, 1H), 7.12 (d, *J* = 8.2 Hz, 1H), 4.31 (t, *J* = 7.2 Hz, 2H), 3.08 (t, *J* = 7.2 Hz, 2H), 1.05 (s, 9H), 0.25 (s, 6H).

N-{8-[(tert-butyldimethylsilyl)oxy]quinolin-5-yl}-4-{1,1-dioxido-3-oxobenzo[d]isothiazol-2(3H)-yl}butanamide (10j)

White solid (Yield 59%), Mp:98-100□.^{1}H NMR (400 MHz, DMSO) δ 9.87 (s, 1H), 9.34 (d, *J* = 1.8 Hz, 1H), 8.91 (dd, *J* = 4.0, 1.5 Hz, 1H), 8.76 (dd, *J* = 8.4, 2.0 Hz, 1H), 8.42 – 8.35 (m, 2H), 7.58 (dd, *J* = 8.6, 4.1 Hz, 1H), 7.54 (d, *J* = 8.2 Hz, 1H), 7.20 (d, *J* = 8.2 Hz, 1H), 3.93 (t, *J* = 7.0 Hz, 2H), 2.64 (t, *J* = 7.2 Hz, 2H), 2.21 – 2.10 (m, 2H), 1.06 (s, 9H), 0.26 (s, 6H).

N-{8-[(tert-butyldimethylsilyl)oxy]quinolin-5-yl}-5-{1,1-dioxido-3-oxobenzo[d]isothiazol-2(3H)-yl}pentanamide (10k)

White solid (Yield 74%), Mp:120-122□. ^{1}H NMR (400 MHz, DMSO) δ 9.83 (s, 1H), 8.88 (dd, *J* = 4.0, 1.5 Hz, 1H), 8.33 (d, *J* = 8.1 Hz, 2H), 8.13 (d, *J* = 7.3 Hz, 1H), 8.11 – 7.97 (m, 2H), 7.54

(dd, *J* = 8.5, 4.0 Hz, 1H), 7.51 (d, *J* = 8.2 Hz, 1H), 7.17 (d, *J* = 8.2 Hz, 1H), 3.80 (t, *J* = 7.0 Hz, 2H), 1.93 – 1.82 (m, 2H), 1.80 – 1.69 (m, 2H), 1.04 (s, 9H), 0.23 (s, 6H).

N-{8-[(tert-butyldimethylsilyl)oxy]quinolin-5-yl}-6-{1,1-dioxido-3-oxobenzo[d]isothiazol-2(3H)-yl}hexanamide (10l)

White solid (Yield 63%), Mp:118-120□. ^{1}H NMR (400 MHz, $CDCl_3$) δ 8.82 (dd, *J* = 3.9, 1.2 Hz, 1H), 8.09 (dd, *J* = 8.5, 1.2 Hz, 1H), 7.96 (d, *J* = 6.8 Hz, 1H), 7.86 – 7.74 (m, 3H), 7.61 (s, 1H), 7.46 (d, *J* = 8.2 Hz, 1H), 7.34 (dd, *J* = 8.5, 4.1 Hz, 1H), 7.07 (d, *J* = 8.2 Hz, 1H), 3.81 (t, *J* = 7.2 Hz, 2H), 2.46 (t, *J* = 7.4 Hz, 2H), 1.96 – 1.89 (m, 2H), 1.87 – 1.78 (m, 2H), 1.59 – 1.50 (m, 2H), 1.06 (s, 9H), 0.25 (s, 6H).

4.2.3. General procedure for the synthesis of 11a-11l

The solution of **10a** (0.22g) in MeOH(4ml) was acidified by 2M hydrochloric acid solution to pH 2. The mixture was stirred at room temperature for 4h. Saturated aqueous $NaHCO_3$ solution was added and a yellow solid was acquired. The mixture was filtered to get the white solid as the crude product. The crude product was purified by recrystallization (EtOAc) to give the desired product as white solid.

N-(8-hydroxyquinolin-5-yl)-3-[methyl(phenyl)amino]propanamide (11a)

White solid (Yield 61%), Mp:165-168℃. ^{1}H NMR (400 MHz, DMSO) δ 9.82 (s, 1H), 8.85 (dd, *J* = 4.1, 1.5 Hz, 1H), 8.24 (dd, *J* = 8.6, 1.5 Hz, 1H), 7.52 (dd, *J* = 8.6, 4.1 Hz, 1H), 7.40 (d, *J* = 8.2 Hz, 1H), 7.21 (dd, *J* = 8.7, 7.3 Hz, 2H), 7.05 (d, *J* = 8.2 Hz, 1H), 6.81 (d, *J* = 8.0 Hz, 2H), 6.65 (t, *J* = 7.2 Hz, 1H), 3.72 (t, *J* = 7.0 Hz, 2H), 2.94 (s, 3H), 2.66 (t, *J* = 7.0 Hz, 2H). ^{13}C NMR (101 MHz, DMSO) δ 171.22, 151.82, 149.31, 148.50, 138.74, 132.64, 129.53, 124.92, 124.82, 124.59, 121.86, 116.45, 112.82, 110.86, 49.14, 38.29, 33.62. HRMS (ESI) m/z Calcd $[M+H]^+$ 322.1550, found: 322.1541.

N-(8-hydroxyquinolin-5-yl)-4-[methyl(phenyl)amino]butanamide (11b)

White solid (Yield 65%), Mp:177-180℃. ^{1}H NMR (400 MHz, $CDCl_3$) δ 8.76 (d, *J* = 3.4 Hz, 1H), 8.03 (d, *J* = 8.3 Hz, 1H), 7.41 (d, *J* = 7.9 Hz, 2H), 7.30 (s, 1H), 7.23 (d, *J* = 7.7 Hz, 2H), 7.11 (d, *J* = 8.0 Hz, 1H), 6.78 (d, *J* = 8.2 Hz, 2H), 6.72 (t, *J* = 7.2 Hz, 1H), 3.46 (t, *J* = 6.9 Hz, 2H), 2.95 (s, 3H), 2.53 (t, *J* = 7.0 Hz, 2H), 2.16 – 2.05 (m, 2H). ^{13}C NMR (101 MHz, DMSO) δ 172.27, 151.79, 149.54, 148.51, 138.76, 132.57, 129.48, 124.99, 124.92, 124.67, 121.91, 115.98, 112.37, 110.90, 51.84, 38.33, 33.26, 22.56. HRMS (ESI) m/z Calcd $[M+H]^+$ 336.1706, found: 336.1698.

N-(8-hydroxyquinolin-5-yl)-5-[methyl(phenyl)amino]pentanamide (11c)

White solid (Yield 51%), Mp:123-126℃. ^{1}H NMR (400 MHz, $CDCl_3$) δ 8.78 (d, *J* = 3.6 Hz, 1H), 8.06 (d, *J* = 8.3 Hz, 1H), 7.44 (d, *J* = 7.9 Hz, 2H), 7.22 (d, *J* = 7.7 Hz, 2H), 7.17 – 7.10 (m, 2H), 6.73 (d, *J* = 8.3 Hz, 2H), 6.69 (t, *J* = 7.3 Hz, 1H), 3.40 (t, *J* = 7.0 Hz, 2H), 2.95 (s, 3H), 2.50 (t, *J* = 7.2 Hz, 2H), 1.89 – 1.79 (m, 2H), 1.77 – 1.68 (m, 2H). ^{13}C NMR (101 MHz, $CDCl_3$) δ 172.46, 151.17, 149.28, 147.88, 138.08, 131.48, 129.27, 125.22, 124.55, 123.23, 121.84, 116.20, 112.28, 109.25, 52.44, 38.48, 36.63, 26.53, 23.45. HRMS (ESI) m/z Calcd $[M+H]^+$ 350.1863, found: 350.1858.

N-(8-hydroxyquinolin-5-yl)-6-[methyl(phenyl)amino]hexanamide (11d)

White solid (Yield 55%), Mp:132-135℃. ^{1}H NMR (400 MHz, $CDCl_3$) δ 8.78 (d, *J* = 3.4 Hz, 1H), 8.10 (d, *J* = 8.3 Hz, 1H), 7.46 (d, *J* = 7.1 Hz, 2H), 7.25 – 7.20 (m, 2H), 7.13 (d, *J* = 7.5 Hz, 1H), 6.71 (d, *J* = 8.5 Hz, 2H), 6.67 (d, *J* = 7.3 Hz, 1H), 3.35 (t, *J* = 7.3 Hz, 2H), 2.93 (s, 3H), 2.48 (t, *J* = 7.3 Hz, 2H), 1.91 – 1.79 (m, 2H), 1.71 – 1.63 (m, 2H), 1.51 – 1.44 (m, 2H). ^{13}C NMR (101 MHz, DMSO) δ 172.48, 151.73, 149.51, 148.49, 138.75, 132.50, 129.47, 124.95, 124.62, 121.89, 115.83, 112.32, 110.89, 52.14, 38.37, 36.13, 26.76, 26.27, 25.74. HRMS (ESI) m/z Calcd $[M+H]^+$ 364.2019, found: 364.1997.

N-(8-hydroxyquinolin-5-yl)-3-{2-methyl-1H-benzo[d]imidazol-1-yl}propanamide (11e)

White solid (Yield 57%), Mp:234-236℃.^{1}H NMR (400 MHz, DMSO) δ 9.77 (s, 1H), 8.77 (d, *J* = 3.9 Hz, 1H), 7.76 (d, *J* = 8.5 Hz, 1H), 7.59 – 7.53 (m, 2H), 7.37 (dd, *J* = 8.5, 4.1 Hz, 1H), 7.21 (dd, *J* = 8.5, 4.8 Hz, 1H), 7.19 – 7.12 (m, 2H), 6.94 (d, *J* = 8.2 Hz, 1H), 4.54 (t, *J* = 6.6 Hz, 2H), 2.94 (t, *J* = 6.6 Hz, 2H), 2.58 (s, 3H), 2.09 (s, 1H). ^{13}C NMR (101 MHz, DMSO) δ 170.05, 152.36, 152.28, 148.43, 142.93, 138.79, 135.39, 132.31, 124.90, 124.72, 124.15, 121.88, 121.77, 121.68, 118.64, 110.85, 110.66, 36.04, 14.01. HRMS (ESI) m/z Calcd $[M+H]^+$ 347.1502, found: 347.1504.

N-(8-hydroxyquinolin-5-yl)-4-{2-methyl-1H-benzo[d]imidazol-1-yl}butanamide (11f)

White solid (Yield 69%), Mp:217-220℃. ^{1}H NMR (400 MHz, $CDCl_3$) δ 9.71 (s, 1H), 8.77 (d, *J* = 3.2 Hz, 1H), 8.19 (d, *J* = 8.2 Hz, 1H), 7.52 – 7.41 (m, 3H), 7.35 (d, *J* = 8.2 Hz, 1H), 7.15 – 7.03 (m, 2H), 6.98 (d, *J* = 8.2 Hz, 1H), 4.20 (t, *J* = 7.2 Hz, 2H), 2.50 (s, 3H), 2.43 (d, *J* = 4.7 Hz, 2H), 2.09 – 1.98 (m, 2H). ^{13}C NMR (101 MHz, DMSO) δ 171.73, 152.13, 151.87, 148.51, 142.86, 138.77, 135.65, 132.59, 124.97, 124.77, 124.66, 121.90, 121.88, 121.59, 118.67, 110.90, 110.29, 43.04, 32.59, 25.45, 13.95. HRMS (ESI) m/z Calcd $[M+H]^+$ 361.1659, found: 361.1638.

N-(8-hydroxyquinolin-5-yl)-5-{2-methyl-1H-benzo[d]imidazol-1-yl}pentanamide (11g)

White solid (Yield 45%), Mp:197-200℃. ^{1}H NMR (400 MHz, DMSO) δ 9.66 (s, 1H), 8.75 (dd, *J* = 4.0, 1.2 Hz, 1H), 8.13 (dd, *J* = 8.5, 1.3 Hz, 1H), 7.46 – 7.39 (m, 3H), 7.30 (d, *J* = 8.2 Hz, 1H), 7.05 (td, *J* = 6.9, 1.0 Hz, 2H), 6.94 (d, *J* = 8.2 Hz, 1H), 4.13 (t, *J* = 7.1 Hz, 2H), 2.45 (s, 3H), 2.39 – 2.34 (m, 2H), 1.77 – 1.66 (m, 2H), 1.62 – 1.54 (m, 2H). ^{13}C NMR (101 MHz, DMSO) δ 172.22, 152.03, 151.79, 148.51, 142.80, 138.75, 135.63, 132.45, 124.93, 124.83, 124.65, 121.89, 121.82, 121.54, 118.66, 110.89, 110.28, 43.26, 35.64, 29.45, 23.10, 13.99. HRMS (ESI) m/z Calcd $[M+H]^+$ 375.1815, found: 375.1827

N-(8-hydroxyquinolin-5-yl)-6-{2-methyl-1H-benzo[d]imidazol-1-yl}hexanamide (11h)

White solid (Yield 35%), Mp:125-128℃. ^{1}H NMR (400 MHz, DMSO) δ 9.76 (s, 1H), 9.70 (s, 1H), 8.86 (dd, *J* = 4.1, 1.4 Hz, 1H), 8.23 (dd, *J* = 8.6, 1.5 Hz, 1H), 7.56 (dd, *J* = 8.6, 4.1 Hz, 1H), 7.51 (t, *J* = 6.6 Hz, 2H), 7.37 (d, *J* = 8.2 Hz, 1H), 7.19 – 7.10 (m, 2H), 7.03 (d, *J* = 8.2 Hz, 1H), 4.21 (t, *J* = 7.2 Hz, 2H), 2.55 (s, 3H), 2.40 (t, *J* = 7.3 Hz, 2H), 1.83 – 1.73 (m, 2H), 1.72 – 1.65 (m, 2H), 1.43 – 1.35 (m, 2H). ^{13}C NMR (101 MHz, DMSO) δ 172.37, 152.03, 151.74, 148.48, 142.76, 138.72, 135.60, 132.46, 124.93, 124.88, 124.61, 121.89, 121.80, 121.51, 118.62, 110.87, 110.28, 43.40, 35.95, 29.58, 26.43, 25.44, 13.99. HRMS (ESI) m/z Calcd $[M+H]^+$ 389.1972, found: 389.1943.

3-{1,1-dioxido-3-oxobenzo[*d*]isothiazol-2(3*H*)-yl}-*N*-(8-hydroxyquinolin-5-yl)propanamide (11i)

White solid (Yield 38%), Mp:210-213℃.^{1}H NMR (400 MHz, DMSO) δ 9.93 (s, 1H), 8.85 (dd, *J* = 4.0, 1.4 Hz, 1H), 8.39 – 8.31 (m, 2H), 8.15 (d, *J* = 7.6 Hz, 1H), 8.11 – 8.05 (m, 1H), 8.02 (t, *J* = 7.1 Hz, 1H), 7.54 (dd, *J* = 8.6, 4.1 Hz, 1H), 7.45 (d, *J* = 8.2 Hz, 1H), 7.04 (d, *J* = 8.2 Hz, 1H), 4.10 (t, *J* = 7.3 Hz, 2H), 2.97 (t, *J* = 7.3 Hz, 2H). ^{13}C NMR (101 MHz, DMSO) δ 169.32, 158.93, 152.08, 148.47, 138.78, 137.34, 136.31, 135.77, 132.68, 126.84, 125.58, 124.96, 124.72, 124.43, 122.04, 121.85, 110.86, 35.63, 34.76. HRMS (ESI) m/z Calcd $[M+H]^+$ 398.1702, found: 398.1711

4-{1,1-dioxido-3-oxobenzo[*d*]isothiazol-2(3*H*)-yl}-*N*-(8-hydroxyquinolin-5-yl)butanamide (11j)

White solid (Yield 40%), Mp:221-223℃. ^{1}H NMR (400 MHz, DMSO) δ 9.77 (d, 2H), 9.30 (s, 1H), 8.86 (d, *J* = 4.0 Hz, 1H), 8.73 (d, 1H), 8.41 – 8.26 (m, 2H), 7.58 (dd, *J* = 8.6, 4.1 Hz, 1H), 7.43 (d, *J* = 8.2 Hz, 1H), 7.04 (d, *J* = 8.0 Hz, 1H), 3.89 (t, 2H), 2.59 (t, *J* = 7.3 Hz, 2H), 2.18 – 2.06 (m, 2H). ^{13}C NMR (101 MHz, DMSO) δ 171.53, 157.61, 152.27, 151.81, 148.51, 138.74, 138.13, 132.65, 131.61, 130.75, 127.27, 124.99, 124.85, 124.63, 121.90, 118.48, 110.88, 32.77, 24.32. HRMS (ESI) m/z Calcd $[M+H]^+$ 412.0961, found: 412.0950.

5-{1,1-dioxido-3-oxobenzo[*d*]isothiazol-2(3*H*)-yl}-*N*-(8-hydroxyquinolin-5-yl)pentanamide (11k)

White solid (Yield 46%), Mp:152-154℃. ^{1}H NMR (400 MHz, DMSO) δ 9.76 (d, *J* = 2.7 Hz, 2H), 8.86 (dd, *J* = 4.1, 1.5 Hz, 1H), 8.37 – 8.25 (m, 2H), 8.13 (d, *J* = 7.5 Hz, 1H), 8.10 – 7.97 (m, 2H), 7.57 (dd, *J* = 8.6, 4.1 Hz, 1H), 7.42 (d, *J* = 8.2 Hz, 1H), 7.04 (d, *J* = 8.2 Hz, 1H), 3.79 (t, *J* = 7.1 Hz, 2H), 2.48 (t, *J* = 7.0 Hz, 2H), 1.90 – 1.80 (m, 2H), 1.81 – 1.67 (m, 2H). ^{13}C NMR (101 MHz, DMSO) δ 172.17, 159.09, 151.76, 148.50, 138.74, 137.26, 136.24, 135.73, 132.58, 126.82, 125.54, 124.98, 124.90, 124.65, 121.99, 121.91, 110.87, 39.03, 35.48, 28.08, 23.03. HRMS (ESI) m/z Calcd $[M+H]^+$ 426.1118, found: 426.1105.

6-{1,1-dioxido-3-oxobenzo[*d*]isothiazol-2(3*H*)-yl}-*N*-(8-hydroxyquinolin-5-yl)hexanamide (11l)

White solid (Yield 44%), Mp:143-146℃. ^{1}H NMR (400 MHz, $CDCl_3$) δ 8.76 (d, *J* = 3.5 Hz, 1H), 8.11 (d, *J* = 8.5 Hz, 1H), 7.95 (d, *J* = 6.7 Hz, 1H), 7.86 – 7.74 (m, 3H), 7.49 – 7.41 (m, 2H), 7.38 (s, 1H), 7.08 (d, *J* = 8.1 Hz, 1H), 3.85 (t, *J* = 7.0 Hz, 2H), 2.50 (t, *J* = 7.3 Hz, 2H), 1.99 – 1.92 (m, 2H), 1.93 – 1.85 (m, 2H), 1.62 – 1.55 (m, 2H). ^{13}C NMR (101 MHz, DMSO) δ 172.39, 159.09, 151.72, 148.47, 138.72, 137.26, 136.25, 135.73, 132.56, 126.78, 125.53, 124.99, 124.94, 124.66, 121.98, 121.89, 110.85, 39.17, 35.91, 28.20, 26.34, 25.27. HRMS (ESI) m/z Calcd $[M+H]^+$ 440.1274, found: 412.1259.

4.3. Colorimetric Screening against MMP-2 and MMP-9.

MMP-2 and MMP-9 inhibitory activities of all target compounds were evaluated by MMP-2 and MMP-9 Colorimetric Drug Discovery Kit (BML-AK408, BML-AK410, Enzo®Life Sciences). All assays were carried out in clear Costar 96-well, half-area, flat-bottom assay plates. Each well contained a total volume of 90μL including 50μL assay buffer, 20μL human recombinant MMP-2

or MMP-9 and 20μL test inhibitors. The enzymes were not added to the blanks and the test inhibitors were not added to the controls. After a 30 min incubation period at 37 °C, the reaction was initiated by the addition of 10 μL of chromogenic MMP substrate. Absorbance was monitored at 412 nm using a microtiterplate reader, and measurements were recorded every minute for 20 min.

4.4. Molecular docking

Surflex-dock program in Sybyl-X 2.1.1 was used with default values for all docking studies. Ligands were optimized using concord method and assigned with Gasteiger-Hückel charges. The structure of MMP-2 and MMP-9 was downloaded from the Protein Data Bank server with PDB code: 1HOV and 1GKC. The top-scored pose of selected compounds were selected as the representative structures.

4.5. MTT assay

All cell lines were cultured in RPMI1640 medium (10% FBS) at 37°C in a 5% CO_2 humidified incubator. Briefly, Cancer cells were plated at 4000-5000 cells per well (100μL/well) in 96-well plates for 8 h and then treated with different concentrations of compounds (100μL/well) for 48 h. 0.5% MTT solution (10μL/well) was added and incubation for 4 h. DMSO (150μL/well) was added to extract formazan formed from MTT. Absorbance was determined using a microtiter-plate reader at 570 nm. The IC_{50} values were calculated according to the inhibition ratios.

4.6. Cell migration and invasion assay

A549 cell was plated at 200,000 cells per well (1000μL/well) in 12-well plates for 8 h and then treated with compound **5e** or **5h** (1000μL/well) for 24 h. Then cells were harvested and resuspended as single cells in 1000μL serum-free RPMI1640.

For the migration experiments, we took 30,000 cells in 200μL serum-free RPMI1640. Cells were added to the upper chamber and the lower chamber was filled with 600μL RPMI1640 supplemented with 10% FBS. Cells were allowed to migrate for 24 h at 37°C in a 5% CO_2 humidified incubator. The experiment was terminated by discarding the medium and fixing the cells with MeOH/Acetic acid (3:1) for 20 min. Non-invading cells on the upper side of the insert were removed by a cotton-tipped applicator. Staining of the cells on the bottom of the membrane was performed with crystal violet (0.1%) for 20 min at room temperature and washed with PBS. Then lower surface was captures and counted. Cells were either counted manually or with the help of the Image J software.

For the invasion experiments, the chamber membrane was covered with 50μL matrigel (1:10 diluted) for 2 hours at 37°C and the rest of the protocol was identical to that described in the migration assay.

4.7. HUVECs tuber formation assay

HUVEC were plated at 200,000 cells per well (1000μL/well) in 12-well plates for 8h and then treated with compound **5e** or **5h** (1000μL/well) for 24h using serum-free RPMI1640. Then cells were harvested and resuspended as single cells in 1000μL serum-free RPMI1640.

The wells of 96-well plates were covered with 100μL matrigel (no diluting) for 2 hours at 37°C. Then cells were carefully layered on the top of the polymerized matrigel. After 6h incubation on

matrigel, the dimensional organization of the cells was examined under an inverted microscope. The number of meshes where measured as a direct parameter for HUVEC angiogenesis efficiency, using the Angiogenesis tool and Image J software.

4.8. Apoptosis Assay.

A549 cells (1×10^5 cells/mL) were seeded in 12-well plates and treated with compounds **5e**, **5h** and **A** of 1, 5 and 10 μM for 48h. The cells were then harvested and washed with cold PBS. After the centrifugation and removal of the supernatants, cells were resuspended in 200 μL of binding buffer, which was then added to 5μL of annexin V-FITC and 10μL of PI. Then the cells were incubated at room temperature for another 15min in the dark. The stained cells were analyzed by a flow cytometer.

4.9. Western blot

A549 cells were treated with **5e, 5h** and **A** for 24h. The assay protocol has been described previously [26]. Cell lysates were prepared using SDS-PAGE loading bu□er and subjected to SDS-PAGE, they were then transferred to PVDF membranes using the Trans-Blot Turbo Transfer system (Bio-Rad). After blocking with 10% dry milk in TBST, membranes were probed with rabbit anti-MMP-2, rabbit anti-MMP-9 or rabbit anti-GAPDH antibody, then were incubated with secondary antibodies. Images were acquired using Amersham Imager 680.

Zymography in 10% polyacrylamide gel containing 0.1% gelatin was performed according to the earlier method[27]. Gelatin was used to detect MMP-2 and MMP-9 activity in the culture medium. Cell supernatants were electrophoresed on an 8% SDS-PAGE containing 2% gelatin. The gels were washed with 0.25% triton three times. Then the gels were cut and incubated in the zymography buffer (0.15 M NaCl, 5 mM $CaCl_2$, 0.05% NaN_3 and 50 mM Tris-HCl buffer, pH 7.5) at 37°C for 48 h. After incubation, the gels were stained with 0.25% Coomassie Brilliant Blue R250, and detained with acetic acid, methanol and water. MMP activity was represented by a white band of gelatin digestion.

Acknowledgments

This work was supported by National Natural Science Foundation of China (81874288 and 21672127), Key Research and Development Project of Shandong Province (Grant No. 2017CXGC1401), the Fundamental Research Funds of Shandong University (Grant No. 2019GN045) and The Joint Research Funds for Shandong University and Karolinska Institute (SDU-KI-2019-06).

References

[1] C.A. Kontogiorgis, P. Papaioannou, D.J. Hadjipavlou-Litina, Matrix metalloproteinase inhibitors: a review on pharmacophore mapping and (Q)SARs results, Curr. Med. Chem., 12 (2005) 339-355.

[2] M. Nakamura, S. Miyamoto, H. Maeda, G. Ishii, T. Hasebe, T. Chiba, M. Asaka, A. Ochiai, Matrix metalloproteinase-7 degrades all insulin-like growth factor binding proteins and facilitates insulin-like growth factor bioavailability, Biochem. Biophys. Res. Commun., 333 (2005) 1011-1016.

[3] M. Tian, J.R. Neil, W.P. Schiemann, Transforming growth factor-β and the hallmarks of cancer, Cell. Signal., 23 (2011) 951-962.

[4] Z. Werb, ECM and Cell Surface Proteolysis: Regulating Cellular Ecology, Cell, 91 (1997) 439-442.
[5] H. Zheng, H. Takahashi, Y. Murai, Z. Cui, K. Nomoto, H. Niwa, K. Tsuneyama, Y. Takano, Expressions of MMP-2, MMP-9 and VEGF are closely linked to growth, invasion, metastasis and angiogenesis of gastric carcinoma, Anticancer Res., 26 (2006) 3579-3583.
[6] J.E. Rundhaug, Matrix metalloproteinases and angiogenesis, J. Cell. Mol. Med., 9 (2005) 267-285.
[7] G. Bergers, R. Brekken, G. McMahon, T.H. Vu, T. Itoh, K. Tamaki, K. Tanzawa, P. Thorpe, S. Itohara, Z. Werb, D. Hanahan, Matrix metalloproteinase-9 triggers the angiogenic switch during carcinogenesis, Nat. Cell Biol., 2 (2000) 737-744.
[8] J. Fang, Y. Shing, D. Wiederschain, L. Yan, C. Butterfield, G. Jackson, J. Harper, G. Tamvakopoulos, M.A. Moses, Matrix metalloproteinase-2 is required for the switch to the angiogenic phenotype in a tumor model, Proc. Natl. Acad. Sci. U. S. A., 97 (2000) 3884-3889.
[9] A. Mukherjee, N. Adhikari, T. Jha, A pentanoic acid derivative targeting matrix metalloproteinase-2 (MMP-2) induces apoptosis in a chronic myeloid leukemia cell line, Eur. J. Med. Chem., 141 (2017) 37-50.
[10] C. Daniel, J. Duffield, T. Brunner, K. Steinmann-Niggli, N. Lods, H.P. Marti, Matrix metalloproteinase inhibitors cause cell cycle arrest and apoptosis in glomerular mesangial cells, J. Pharmacol. Exp. Ther., 297 (2001) 57-68.
[11] O. Nyormoi, L. Mills, M. Bar-Eli, An MMP-2/MMP-9 inhibitor, 5a, enhances apoptosis induced by ligands of the TNF receptor superfamily in cancer cells, Cell Death Differ., 10 (2003) 558-569.
[12] D. Bissett, K.J. O'Byrne, J. von Pawel, U. Gatzemeier, A. Price, M. Nicolson, R. Mercier, E. Mazabel, C. Penning, M.H. Zhang, M.A. Collier, F.A. Shepherd, Phase III study of matrix metalloproteinase inhibitor prinomastat in non-small-cell lung cancer, J. Clin. Oncol., 23 (2005) 842-849.
[13] V. Oliveri, G. Vecchio, 8-Hydroxyquinolines in medicinal chemistry: A structural perspective, Eur. J. Med. Chem., 120 (2016) 252-274.
[14] S.R. Bareggi, U. Cornelli, Clioquinol: Review of its Mechanisms of Action and Clinical Uses in Neurodegenerative Disorders, 18 (2012) 41-46.
[15] J.A. Jacobsen, J.L. Fullagar, M.T. Miller, S.M. Cohen, Identifying chelators for metalloprotein inhibitors using a fragment-based approach, J. Med. Chem., 54 (2011) 591-602.
[16] T.S. Rush, 3rd, R. Powers, The application of x-ray, NMR, and molecular modeling in the design of MMP inhibitors, Curr. Top. Med. Chem., 4 (2004) 1311-1327.
[17] E. Attolino, V. Calderone, E. Dragoni, M. Fragai, B. Richichi, C. Luchinat, C. Nativi, Structure-based approach to nanomolar, water soluble matrix metalloproteinases inhibitors (MMPIs), Eur. J. Med. Chem., 45 (2010) 5919-5925.
[18] X. Jin, Z. Yang, T. Li, B. Wang, Y. Li, M. Yan, C. Liu, J. An, 8-hydroxyquinoline-5-carbaldehyde-(benzotriazol-1'-acetyl)hydrazone as a potential Mg2+ fluorescent chemosensor, J. Coord. Chem., 66 (2013) 300-305.
[19] A. Hazra, Y.P. Bharitkar, A. Maity, S. Mondal, N.B. Mondal, Synthesis of tetracyclic pyrrolidine/isoxazolidine fused pyrano[3,2-h]quinolines via intramolecular 1,3-dipolar cycloaddition in ionic liquid, Tetrahedron Lett., 54 (2013) 4339-4342.
[20] J. Murray, D. Nowak, L. Pukenas, R. Azhar, M. Guillorit, C. Walti, K. Critchley, S. Johnson, R.S. Bon, Solid phase synthesis of functionalised SAM-forming alkanethiol-oligoethyleneglycols, Journal of materials chemistry. B, 2 (2014) 3741-3744.
[21] S.S. Chhajed, P. Manisha, V.A. Bastikar, H. Animeshchandra, V.N. Ingle, C.D. Upasani, S.S.

Wazalwar, Synthesis and molecular modeling studies of 3-chloro-4-substituted-1-(8-hydroxy-quinolin-5-yl)-azetidin-2-ones as novel anti-filarial agents, Bioorg. Med. Chem. Lett., 20 (2010) 3640-3644.

[22] X. Yan, Y. Yu, P. Ji, H. He, C. Qiao, Antitumor activity of endoperoxide-iron chelator conjugates-design, synthesis and biological evaluation, Eur. J. Med. Chem., 102 (2015) 180-187.

[23] L.J. MacPherson, E.K. Bayburt, M.P. Capparelli, B.J. Carroll, R. Goldstein, M.R. Justice, L. Zhu, S. Hu, R.A. Melton, L. Fryer, R.L. Goldberg, J.R. Doughty, S. Spirito, V. Blancuzzi, D. Wilson, E.M. O'Byrne, V. Ganu, D.T. Parker, Discovery of CGS 27023A, a non-peptidic, potent, and orally active stromelysin inhibitor that blocks cartilage degradation in rabbits, J. Med. Chem., 40 (1997) 2525-2532.

[24] P.D. Brown, R.E. Bloxidge, N.S. Stuart, K.C. Gatter, J. Carmichael, Association between expression of activated 72-kilodalton gelatinase and tumor spread in non-small-cell lung carcinoma, J. Natl. Cancer Inst., 85 (1993) 574-578.

[25] B.J. Lim, S.S. Jung, S.Y. Choi, C.S. Lee, Expression of metastasis-associated molecules in non-small cell lung cancer and their prognostic significance, Mol Med Rep, 3 (2010) 43-49.

[26] D. Cuffaro, E. Nuti, V. Gifford, N. Ito, C. Camodeca, T. Tuccinardi, S. Nencetti, E. Orlandini, Y. Itoh, A. Rossello, Design, synthesis and biological evaluation of bifunctional inhibitors of membrane type 1 matrix metalloproteinase (MT1-MMP), Biorg. Med. Chem., 27 (2019) 196-207.

[27] C. Medina, S. Videla, A. Radomski, M.W. Radomski, M. Antolin, F. Guarner, J. Vilaseca, A. Salas, J.R. Malagelada, Increased activity and expression of matrix metalloproteinase-9 in a rat model of distal colitis, Am. J. Physiol. Gastrointest. Liver Physiol., 284 (2003) G116-122.

Highlights

1. Thirty-one 8-hydroxyquinoline derivatives were designed and synthesized.

2. Compounds **5e** and **5h** show good MMP-2/9 inhibitory activity.

3. Compounds **5e** and **5h** exert good anti-proliferative, anti-invasive and anti-angiogenetic activity.

4. Compounds **5e** and **5h** down-regulate expression of MMP-2 and MMP-9.